Dissertation for the Master Degree of
Landscape Architecture

Flood Risk Assessment by Estimating Flood Depth Considering Uncertainties in Climate Change

기후변화의 불확실성을 고려한 침수심에 따른 침수위험도 평가

August 2015

Graduate School of Seoul National University

Department of Landscape Architecture and
Rural System Engineering

Ji Yeon Kim

Abstract

Flood Risk Assessment by Estimating Flood Depth Considering Uncertainties in Climate Change

Jiyeon Kim
Landscape Architecture and Rural System Engineering
Graduate school of Agriculture and Life Science
Seoul National University
Academic advisor: Dongkun Lee

A natural risk common in urban areas, flooding caused by localized heavy rain has shown an increase under climate change. Flood risk must be considered from the initial stages of urban planning because of limited expansion in developed areas. However, few studies have attempted to quantify flood risk under uncertainties for land use planning. In addition, most models used to derive flood depth are usually complicated and are not easily employed by land use planners. Therefore, the objectives of this study are to develop a predictive model for flood depth and assess flood risk considering the uncertainties of precipitation in a future climate scenario.

Gimpo city for the study site is prone to flooding and includes large areas under development. This study is presented in four parts. First, Monte Carlo simulation is conducted to create ensemble Representative Concentration Pathway (RCP) scenarios for considering uncertainties of

precipitation. Second, multi-regression analysis was performed to define the flood depth. Third, the flood susceptibility was estimated by using Maximum Entropy (MaxEnt) modeling software. Finally, a flood risk map is derived by superposing the flood depth map in 2050 onto the flood susceptibility map.

The result of ensemble scenarios derived from Monte Carlo simulation indicated an increase in extreme rainfall in 2050. Moreover, the maximum precipitation of daily and accumulated precipitation are expected to increase as much as 106.76 mm and 55.66 mm, respectively, compared with current conditions.

A predictive model for flood depth was derived with independent variables of daily precipitation, accumulated precipitation, relative elevation to the nearest stream, and Topographic Position Index (TPI). The flood depth caused by daily precipitation of extreme rainfall would be 0.01-0.05 m at the safest areas and 1.64-2.34 m at the most vulnerable areas. The flood depth would be significantly higher in the case of accumulated precipitation.

Flood susceptibility was divided into eight classes representing areas vulnerable to floods according to environmental conditions. The areas of classes 5 to 8, flood susceptible areas, would account for 28% in Gimpo. Areas with flood depth over 1.0 m, Class 7, are expected to cover 7,200 m^2 . Such areas may be vulnerable for all land use type and thus should not be developed.

This study is significant because land use planners can use the results to establish decision-making criteria for reasonable planning. In the new paradigm of land use planning under climate change, this study can be used as a basic research guide for determining the installation of adaptation strategies to land use allocation.

.....

■ Keywords: Flood depth, Flood susceptibility, Probability distribution of precipitation, Extreme rainfall, Adaptation to flood, Spatial planning

■ Student number: 2013-21146

Table of Contents

List of Figures

List of Tables

I. Introduction

Natural hazards such as flooding have recently been attributed to the impacts of climate change. Urban areas with high populations are particularly vulnerable to these hazards and will be damaged gradually under climate change (Park et al., 2012; Huong and Pathirana, 2013). In South Korea, many urban areas such as Gwanghwa-moon and Gangnam station are prone to flooding through increases in the frequency of localized heavy rain caused by climate change (Ministry of Environment, 2011).

In response, the "safe cities" concept has been developed in land use planning for adaptation to hazards. The Climate-Friendly Safe City Project in Korea revealed that many effects such as variable precipitation and increases in temperature and sea level should be considered when planning cities (National Institute of Environmental Research, 2012). The Ministry of Land, Infrastructure and Transport (2011) also considers the results of vulnerability assessment under climate change in the future when planning urban land use. A "resilient city" similar in concept to city adaptation under climate change, incorporates the risk of natural hazard in land use planning to reduce damages (Storch et al., 2011; UNISDR, 2012).

In order to plan safer cities considering climate change in the future, the impacts caused by climate change should be quantified with various scenarios. When adapting to urban

flooding, quantitative precipitation forecasting and an understanding the trend changes compared with current conditions are critical. Determination of changes in climate elements is key for understanding and mitigating natural hazards under climate change.

However, uncertainties in climate change should be considered in order to derive reliable results. The uncertainties may be defined from natural, social, and human life systems (Walker et al., 2003). Because climate change includes all changes of the systems, various uncertainties can arise. Thus, the uncertainties caused by impacts of climate change should be considered for hazard and risk assessment; such a model can be an effective decision-making tool supporting spatial planning for climate adaptive cities. For risk assessment considering the uncertainties, it is necessary to integrate the possibility of hazard occurrence and its consequences. According to the Intergovernmental Panel on Climate Change (IPCC) 5th assessment report, risk under climate change is assessed from hazard occurrences in addition to their intensities.

Many studies have estimated flood risk; however, limited attempts have been made to quantitatively analyze potential flood areas, flood depth, and flood susceptibility considering the uncertainties in climate change scenarios. In addition, the complicated hydrological model used to quantify flood risk has not been adapted for land use planners.

In this study, flood risk assessment is conducted in the

Gimpo area under four RCP scenarios in 2050. The uncertainties under the scenarios are considered by representing the probability distribution of rainfall events. Moreover, a simple predictive model for flood depth is developed to identify areas vulnerable to flooding. This model can be easily used by land use planners in developing adaptive cities against flood risk. The results of this study can be used as guidelines on managing flood risk and planning safer land use in Gimpo.

II. Literature review

1. Uncertainties in climate change

1.1. Uncertainties from climate scenario and predictive models

Uncertainties exist in every sectors when we are forecasting future. Uncertainties can be divided into two parts: uncertainties from the ignorance and uncertainties from the fluctuation of system. Climate change has both side of uncertainties since the climate change is significantly influenced by both natural and anthropogenic causes (Kim et al., 2014). It is almost impossible to forecast future climate change accurately because of complex systems and unknown variables. A lot of researches have been conducted to set the future climate scenario in various aspects with possible future climate conditions.

Uncertainties from climate change scenario are largely influenced by the assumptions inside the future climate scenario. Using scenario exceeds a range of statistical uncertainties by these large assumptions. The large assumptions cause other assumptions which result expanding of uncertainties. For example, uncertainties are getting larger while forecasting greenhouse gas emission from human activities, and future climate. In the end the impact assessment on the certain sector contains large uncertainties (New and Hulme, 2000).

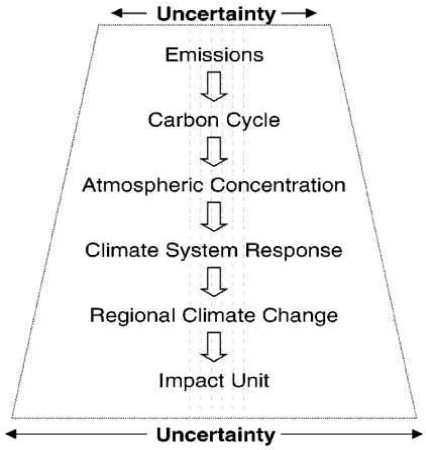

Fig. 1 Uncertainties from climate change impacts (New and Hulme, 2000)

Uncertainties from scenarios explain the possible range of results. However, it is impossible to know the actual possibility of certain events (Walker et al., 2003). IPCC introduced the SRES Scenarios in the late 1990s that focused on global, regional economic growth and environmental protection (IPCC, 2000). In 2010, RCP scenarios were proposed which was linked with climate mitigation action and radiation per square meter (IPCC, 2013). Both scenario sets explain future climate change with possible range of climate in the future. Meanwhile, they could not guarantee which scenario is the most persuadable with quantitative methods.

In addition, Climate models increase uncertainties since they predict different range of precipitation and temperature even in the same climate scenario. There are two types of climate models by its scale GCM (Global/General Circulation

Models) and RCM (Rational Circulation Models). GCMs are models that quantify changes of atmospheric, ocean, polar and terrestrial cycle and processes by atmospheric concentration of greenhouse gases (Mendes and Marengo, 2010). RCMs are specialized models which predict the climate conditions including more regional and high resolution data.

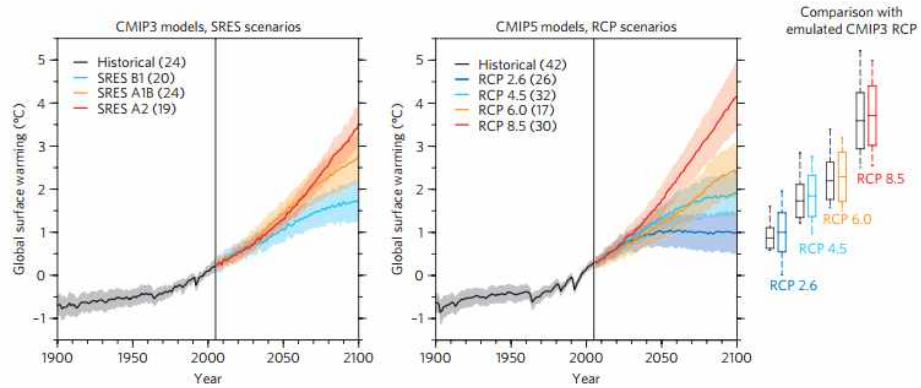

Fig. 2 A range of global surface warming under different scenarios (Knutti and Sedlacek, 2013)

IPCC forecasts future climate change considering uncertainties by using 23 A0GCM (Atmospheric and Oceanic General Circulation Model). On the other hand, multiple GCMs and RCMs are used for forecasting the future precipitation and temperature and representing uncertainties in forecasted outcome (Allen et al., 2000; Tebaldi et al., 2005; Lee et al., 2006; Rauscher et al., 2008; Diallo et al., 2012).

1.2. Handling uncertainties

Climate change has several uncertainties since it has non-linear and dynamic characteristics. Therefore, it is necessary to quantify the uncertainties by the ensemble of various scenarios and climate models. The ensemble models provide a range of uncertainties that supports optimized decision making (Du, 2007). If there are n scenarios and m climate models, n×m outcomes could be derived. these outcomes give the pattern of distribution showing a range of uncertainties. Also, it is possible to use one scenario with m climate model or one climate model with n scenario by the purpose of the prediction.

The ensemble of scenarios or predictive models with probabilistic model is a proper method for considering uncertainties (Tebaldi and Knutti, 2007). The probabilistic model gives detailed information which helps decision making process while the deterministic model does not (Leutbecher and Palmer, 2008). The probabilistic models provide a result from extreme cases and the most frequent cases since they explain future precipitation and temperature by probability distribution.

Monte carlo simulation is generally used for handling uncertainties in climate change by probabilistic model. It is a numerical approach of modeling that can not be done by analytical approach. In order to search numerical solution, monte carlo simulation extracts the probability distribution of variables repetitively with random generation of the values

(Lee and Lee, 2004). In other words, random values are selected from each probability distribution of variable, then they are combined with certain function to derive the probability distribution of a result. As the number of simulation trial increases, the more realistic results can be derived.

Monte carlo simulation provides several advantages. It gives stochastic results showing probable events and each frequencies. Especially, when monte carlo simulation are used in decision making process, uncertainties could be minimized by interpreting characteristics of probability distribution of a result.

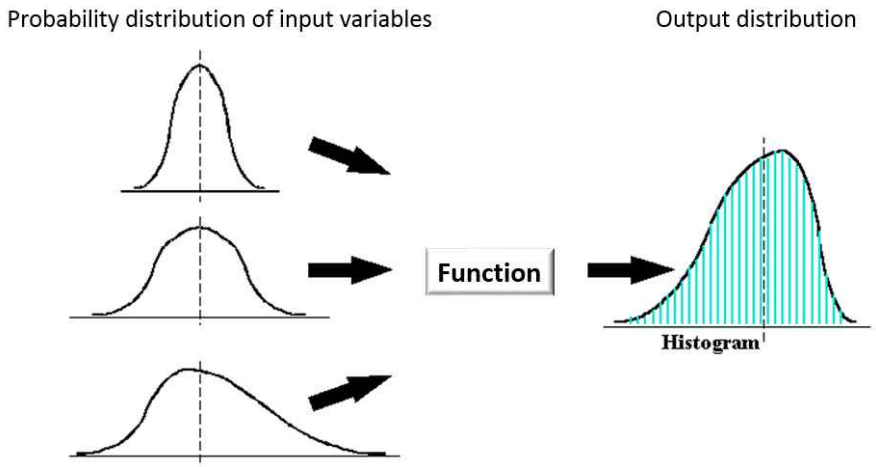

Fig. 3 A concept of Monte Carlo simulation (Cvetko et al., 1998)

Moreover, results from simulation are shown with graph and histogram that helps communication with decision maker. The sensitivity of input variables are clarified as well as the interrelationship among the variables. Also, a combination of

scenarios can be conducted and the results show the changes on the results. In conclusion, monte carlo simulation could provide the pattern of future precipitation considering uncertainties in various scenarios.

2. Flood risk assessment

2.1. Definition and methods of assessment

Risk is defined differently by the each fields of study such as economic risk, environmental risk, ecological risk and engineering risk (Seo, 2011). Climate related risks are derived from the equation with exposure, hazard and vulnerability (Fedeski and Gwilliam, 2007; Foudi et al., 2015). According to IPCC, risk is a combination of extreme weather events, exposure and vulnerability. It could be reduced by management or adaptation strategy to climate change. Risk assessment is conducted for the management of future risk and provide the proper counter measure. Risk can be expressed as equation as below.

$$\text{Risk} = \text{Probability of certain event} \times \text{Its consequences}$$

In other words, the risk can be quantified by the probability of certain event and damage from its consequences. Risk assessment usually is performed on the extreme events such as heat waves, strong wind, heavy rain and landslide.

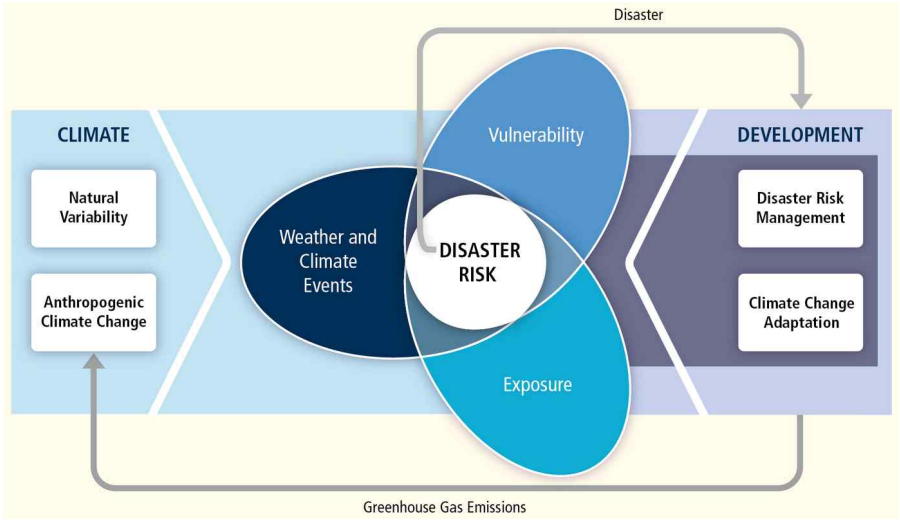

Fig. 4 The concept of risk for assessment and management (IPCC, 2012)

Risk assessment plays an important role in decision making as well as policy making. For the risk assessment, matrix can be used that consist probability of event and its consequences as an effective decision making tool. Then the combination between probability and its consequences can be categorized as degree of risk (Australia, 2009; Queensland, 2011).

Table 1 The Matric of risk assessment (Queensland, 2011)

	Level of negative impact					Level of positive impact				
	Negative consequences					Positive consequences				
Likelihood	Minor	Moderate	Major	Severe	Catastrophic	Minor	Moderate	Major	Severe	Phenomenal
Rare	Low	Low	Low	Low	Low	Low	Low	Low	Low	Low
Unlikely	Low	Low	Medium	Medium	Medium	Low	Low	Medium	Medium	Medium
Possible	Low	Medium	Medium	High	High	Low	Medium	Medium	High	High
Likely	Low	Medium	High	High	Extreme	Low	Medium	High	High	Extreme
Almost certain	Low	Medium	High	Extreme	Extreme	Low	Medium	High	Extreme	Extreme

This method can be applied to the flood risk management as changing future precipitation. Flood risk can be calculated by multiplying probability of flood event and damage from extreme precipitation or probability of extreme precipitation and damage from flood (Moel et al., 2014). Probability of extreme precipitation is calculated from the historical monitoring data and the probability of flood risk is derived from the statistical methods. Flood risk is calculated from the damage cost of flooded areas or the total areas of flooded areas. Damaged areas by flood can be estimated by hydrological models such as SWMM, STROM and MIKEFLOOD. If the damage is defined from cost, the economic loss could be the final output for the risk assessment.

Thus, The risk can be defined from different variables and factors as the purpose of the assessment and characteristics of study site. Generally, the flood risk is defined from duration of precipitation, speed of flood, flooded area and flood depth. Since the flood risk can be divided into inland inundation and river inundation, it is necessary to consider each characteristics of flood risk. The most of urban flood are inland inundation which are caused by the increase of impervious areas and failure of drainage system while flood is caused by river inundation in rural and sub-urban area. Therefore, it is necessary to apply different approach to assess flood risk by the major contribution factors of flood (Korea research institute of human settlement, 2005;

Ministry of Environment, 2011).

Flood risk assessment requires to find out the characteristics of flooded area. Thus, the correlation analysis and regression analysis are used to determine the major vulnerable factors. Then, risk assessment model is made based on those analysis. In order to verify factors which are derived from the correlation analysis, delphi analysis, Analytic Hierachy Process(AHP) method can be used (Joo et al., 2013).

2.2. Flood risk assessment conducted in urban area

Researches on the flood risk assessment have been conducted in many countries. Flood risk is basically calculated with probability of flood event and its consequences, however, factors for the risk assessment depend on the case by case. There are two types of modeling flood risk assessment: hydrological modeling and indices basesd modeling. In this chapter, the methods and factors for the risk assessment used in different countries will be discussed.

Netherlands has been set risk management plan because of vulnerable geographic location where the altitudes are lower than other countries. Netherlands established FLORIS project that assumes weather events happens which exceed the capacity of protection system. The FLORIS project forecasts the flood probability and multiply damage. Damage caused by flood is quantified by calculating casualties, economic cost

and loss of the landscape, wildlife habitat and historical heritages.

United Kingdom also has been conducted researches on the risk assessment framework. Also, UK managed flood event by using flood risk management indices. Flooded area and land use, land cover are used for the flood risk management indices and damage from the flood calculated from the annual economic loss (U.K., 2006). Hydrological indices such as average height, impervious area, water level, standard rate of flow and mean annual precipitation are used for the calculating regional flood risk.

Norway has been working on the mapping frequent flooded area for the flood risk assessment (Norway, 2011). MIKE11 and HEC-RAS are used for simulating flood risk by the changes in precipitation. The hydrological models such as HEC-RAS simulate flow rate, flood depth, flood velocity for the flood prediction (Hydrologic engineering center, 2010). DEM is used as an important variable to detect a location of flooded area in the model.

United State uses similar methodology with Norway to assess flood risk. To operate federal flood insurance program, the areas prone to floods are designated as flood risk districts (US, 2014). FEMA conducts flood risk assessment by using Hazus-MH model. From the flood risk assessment, frequency of precipitation and its annual economic cost are calculated.

South Korea has also tried to conduct risk assessment

since the frequency of urban flood is increasing. Ministry of Environment announced the increased frequency of extreme rainfall and large impervious areas led urban flood after investigating flood characteristics and conditions in Korea. They simulate capacity of drainage system, and then recommend cost-effective flood management in high risk areas. XP-SWMM and MIKEFLOOD are applied for assessment of the flood management by the drainage system.

The Seoul Institute conducted correlation analysis between flood risk assessment and land use pattern to set flood risk management. The elevation, slope, land use and land cover were used for the grouping of flooded areas. The characteristics of 239 drainage areas were used for the correlation analysis. As a result of correlation analysis, the elevation, slope, proportion of urban area and impervious area were considered as significant factors on the urban flood in Seoul. Main factors can be applied for the flood area management at high risk areas.

Table 2 The list of variables used for flood risk assessment

Classification	Variables	Reference
Rainfall	Rainfall intensity (mm/hr)	KRIHS, 2005 SI, 2011
	Daily precipitation	KRIHS, 2005
	Yearly precipitation	KRIHS, 2005 U.K. 2006
	Return periods	Norway, 2011 US, 2014

Topography	Elevation	SI, 2011 ME, 2011 Netherlands, 2005 Norway, 2011 US, 2014 U.K., 2006
	Slope	KRIHS, 2005 SI, 2011 ME, 2011
	TWI (Toographic Wetness Index)	SI, 2011
Land use	Basement	SI, 2011
	areas of each land use	SI, 2011 ME, 2011 U.K., 2006 US, 2014
	Variability	SI, 2011
Land cover	Impervious areas	KRIHS, 2005 SI, 2011 ME, 2011 U.K., 2006
	Building to land ratio	SI, 2011
Infrastructure	Reservoir and drainage systems	KRIHS, 2005 ME., 2011
	Embankment	Netherlands, 2005
Flooded characteristics	Flood depth	ME., 2011
	Flooded areas	ME., 2011
	Flood discharge	ME., 2011 Norway, 2011 US, 2014 U.K., 2006
Damage	loss of life and asset	Netherlands, 2005
	loss of cultural asset and landscape	Netherlands, 2005

III. Research methodology

1. Scope of the study

1.1. Contextual scope

RCP scenarios were used to analyze the change in precipitation in 2050. RCP scenarios describe future climate possibilities depending on atmospheric greenhouse gas (GHG) emissions (IPCC, 2013). The four scenarios, RCP 2.6, 4.5, 6.0, and 8.5, defined by the effectiveness of the mitigation strategy, are named according to radiative forcing values in the mitigation of the following GHG concentrations: +2.6, +4.5, +6.0, and +8.5 W/m2, respectively.

The future precipitation used in this study was derived from HadGEM3-RA high-resolution climate data at 1 km × 1 km. The target year for flood risk assessment was set to 2050, and the representative precipitation data for 2050 was selected from data of 2046-2055. Rainfall intensity (mm/hr) can be important for indicating the characteristics of rainfall; however, forecasts of future rainfall intensity contain huge uncertainties. Therefore, daily precipitation was used for describing the minimum intensity of rainfall rather than hourly rainfall intensity.

Flood depth is one of the most influential factors of flood risk (FEMA, 2014). However, certain areas can show high flood depth at areas in which flooding rarely occurs. Thus, the flood occurrence considering high probability and high

flood depth were determined to derive actual areas having higher risk.

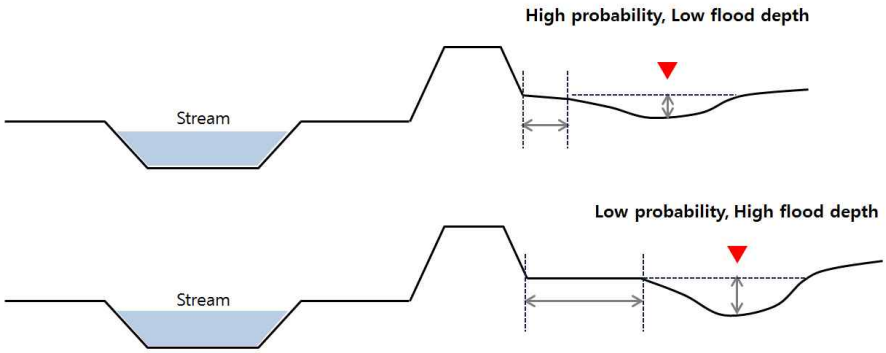

Fig. 5 An example of flood risk as flood depth and flood susceptibility

Flood risk assessment was based on the observed data from areas flooded in 2006, 2008, and 2011. Flooded areas that had not undergone land use change during this period were selected. Moreover, topographic and positional factors were important considerations in the risk assessment because they remained constant during the study period. Variables representing artificial capacity of adaptation were not considered in this study.

1.2. Spatial scope

Gimpo, the study site is prone to flooding and includes large recently developed areas. Choi et al. (2009) identified areas prone to flooding during 2006-2010 and encouraged the use of strategies for adaptation. Because Gimpo was one of the most problematic sites identified in their study, flood risk consideration is needed for safer land use planning in this city.

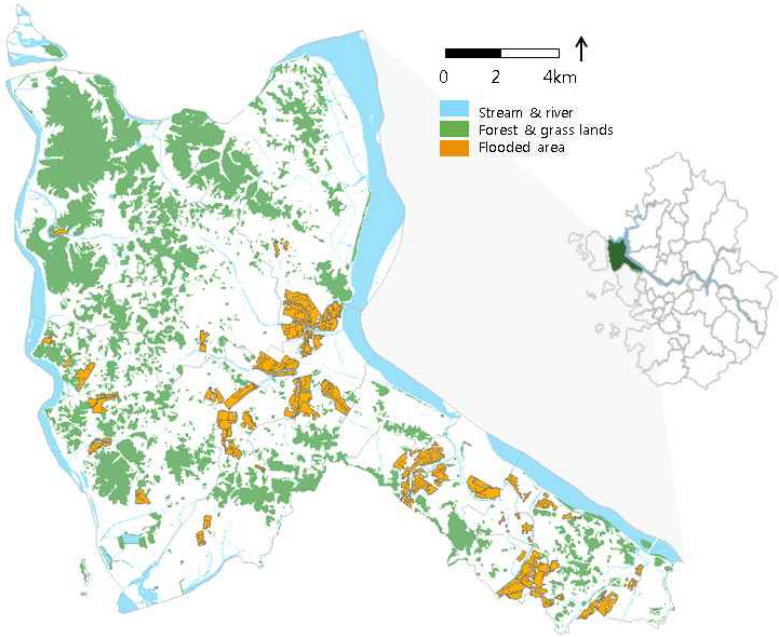

Fig. 6 Gimpo city for study site

The low elevation and gentle slope in Gimpo provide many areas for development. The city is close to capital areas such as Seoul, Incheon, and Bucheon and will be developed gradually through urban planning and management of capital cities as exemplified in the Gyeonggi 2020 project (Gimpo, 2007). In five years, however, Sau and Tongjin have flooded twice; Daegot, Yangchon, and Gochon flooded three times; and Walgot flooded four times.

Recently, large-scale developments such as Yangkok-Masong housing land development and Yangchon industrial park have progressed. Thus, determination of flood risk in Gimpo is crucial for safer land use planning under climate change. The entire region of Gimpo was included in the study site with the exception of the border areas (37° N4

4′ 42″ latitude), which have limited environmental data, and Han-gang River.

2. Methods

This study is divided into three parts. First, the precipitation in 2050, which is a key factor for assessing flood risk, was analyzed. Ensembles of RCP 2.6, 4.5, 6.0, and 8.5 scenarios were conducted, and the probability distribution of extreme rainfall was derived through Monte Carlo simulation. Daily precipitation and three-day accumulated precipitation were also analyzed. From the rainfall distribution, the average and maximum precipitation were defined and compared with current precipitation values.

A predictive model for flood depth and a flood susceptibility map for the probability of flood occurrence were derived. Prediction of flood depth was performed through multi-regression analysis with the environmental variables of flooded areas. The flood susceptibility map was created with Maximum Entropy (MaxEnt) modeling software by extracting similar conditions with flooded areas and searching areas vulnerable to flooding.

Finally, the flood risk map of 2050 was derived by superposing the flood depth map over the flood susceptibility map. The results can be used for political implementation in planning a flood adaptive city.

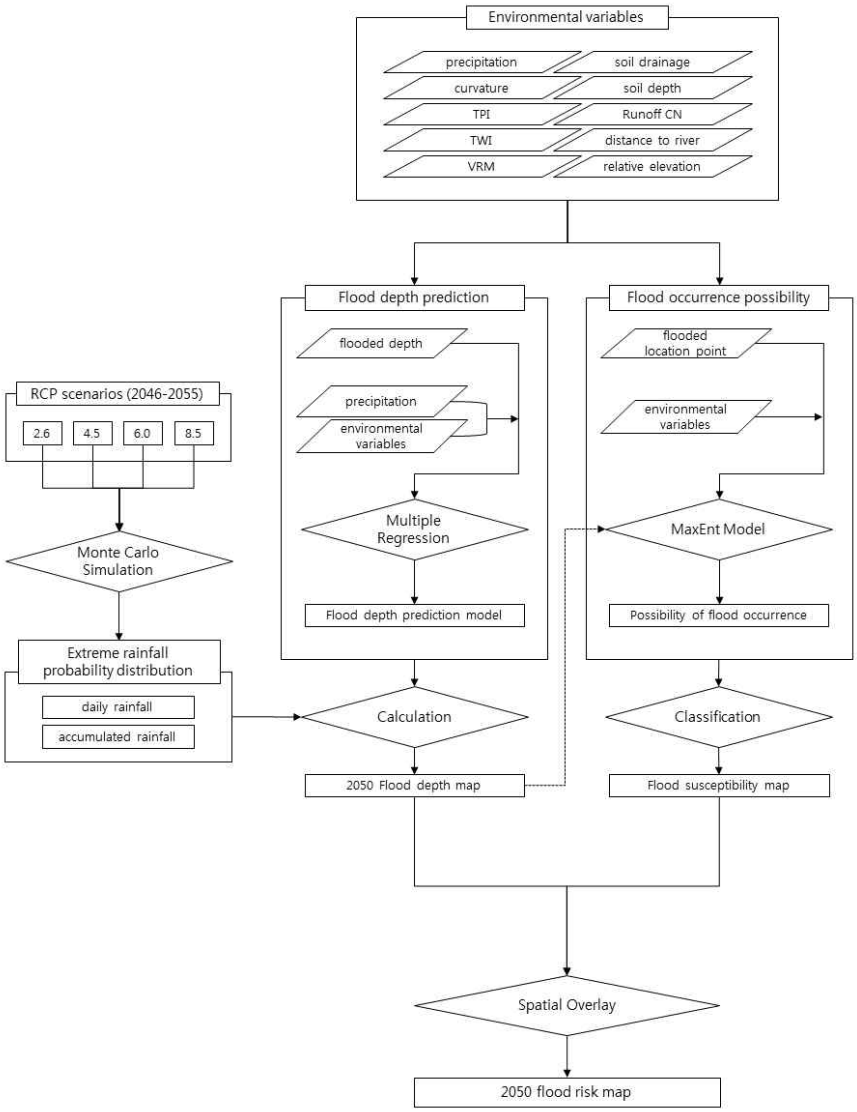

Fig. 7 The research flow

2.1. Changes in precipitation and uncertainties

2.1.1. Changes of rainfall pattern in Gimpo

Before predicting future conditions, the current rainfall pattern must be analyzed. The data of precipitation in Gimpo was collected from Ganghwa Automated Surface Observing System (ASOS), which is the closest station. Ten years of observed data for 2002-2011 was used to create the probability distribution of rainfall events. The frequency of extreme rainfall events was derived in order to compare future precipitation with current patterns.

2.1.2. Ensemble of RCP scenarios by Monte Carlo simulation

The uncertainties in the four RCP scenarios can be considered from the probability distribution of future rainfall, reflecting a range of all scenarios. A Monte Carlo simulation was conducted to establish an ensemble of scenarios from which a range of future precipitation could be defined. Such simulation is used to predict flood depth considering uncertainties in the different scenarios and to provide a quantified result of flood risk.

In order to perform the Monte Carlo simulation, the probability distribution of each scenario should be drawn. Data representative of 2050 was based on daily precipitation and three-day accumulated precipitation predicted from January 1, 2045, to December 31, 2055. A range of extreme rainfall was determined from the minimum precipitation

required to cause flooding in Gimpo. Accordingly, the extreme rainfall was defined as 90 mm in the daily precipitation and 140 mm in the three-day accumulated precipitation. It was assumed that floods would not occur in the condition of precipitation under extreme rainfall.

Monte Carlo simulation was conducted by using Visual Basic for Application (VBA) in Excel with 20,000 iterations. The algorithm was designed to select random values on the probability distribution derived from each of the four scenarios and to calculate the average value among them. The result of simulation was shown as a histogram. Finally, average and maximum precipitation of the scenario ensemble were defined.

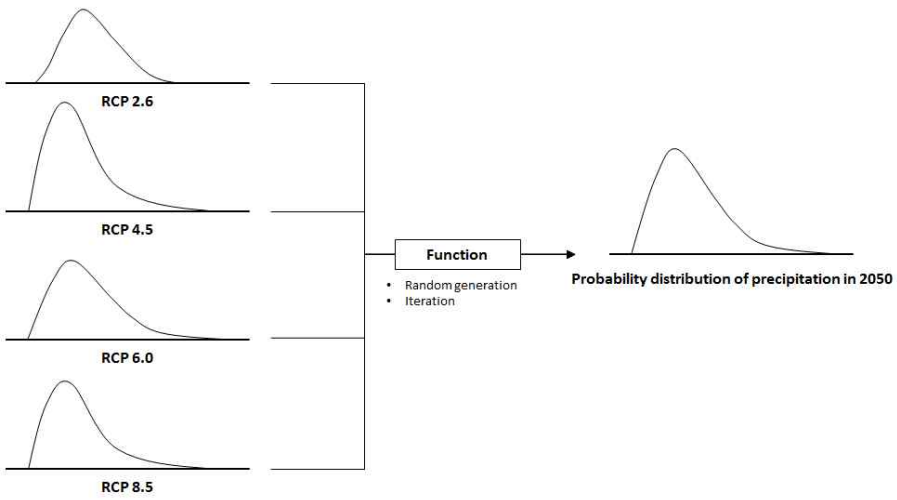

Fig. 8 The probability distribution of future rainfall by Monte Carlo simulation

2.2. Models development for flood risk assessment

2.2.1. Variables in assessment of flood risk

The variables affecting flood depth or flood occurrence were determined through previous research. The precipitation is one of the most influential variables in floods. In this study, daily precipitation and three-day accumulated precipitation were selected to represent rainfall characteristics. Other environmental variables include topographic condition for enabling water to accumulate on the surface, soil and impervious media conditions, which indicate the effect of storm water runoff; and stream condition to consider overflow of streams. These variables were mapped by ArcGIS 10.1.

Table 3 The influential variables to flood occurrence

	Environmental variables	Characteristics
Rainfall	Daily precipitation (mm/day)	Continuous
	3 day accumulated precipitation (mm/3days)	Continuous
Topography	Plan curvature	Continuous
	Profile curvature	Continuous
	Elevation	Continuous
	TPI (Topographic Position Index)	Continuous
	TWI (Topographic Wetness Indes)	Continuous
	VRM (Vector Ruggedness Measure)	Continuous
soil and impervious areas	The capacity of soil drainage	Categorical
	Soil depth	Categorical
	SCS-CN(Curve number)	Continuous
stream	Distance to the nearest stream	Continuous
	Elevation of the nearest stream	Continuous
	Relative elevation of the nearest stream	Continuous

A curvature indicates that water is infiltrated directly into the ground. A high Vector Ruggedness Measure (VRM) value indicates low drainage capacity and thus high vulnerability to floods (Richardson et al., 2001; Nam, 2011). The Topographic Wetness Index (TWI), derived from flow accumulation and slope, affects water storage when the value is higher (Pourali et al., 2014). The Topographic Position Index (TPI) shows whether an elevation is concave or convex at a certain location represented on a grid. A negative TPI indicates that the elevation of a particular area is lower than that of neighboring areas (Jenness, 2006).

$$TWI = \ln\left(\frac{\alpha}{\tan\beta}\right)$$

α = Flow accumulation

β = Slope (rad)

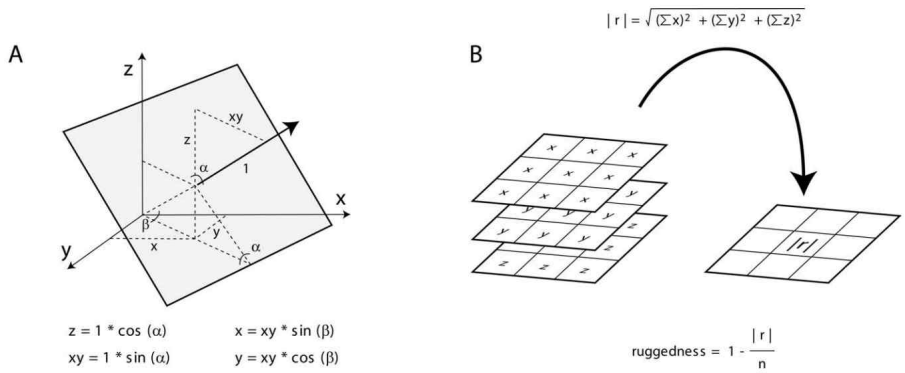

Fig, 9 The process of measuring VRM (Sappington et al., 2005)

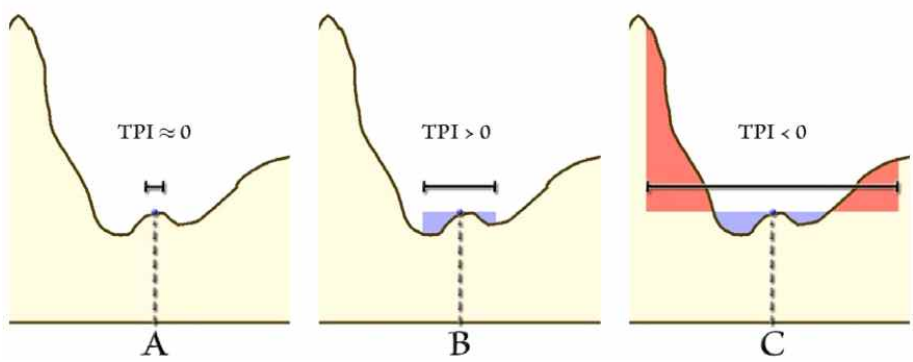

Fig. 10 The concept of TPI (Jenness, 2006)

Considering such variables as topography, infiltration rate, and groundwater level, soil drainage capacity was reclassified into six levels: very good, good, slightly good, slightly poor, poor, and very poor. Soil depth relates to water storage; thus, deeper soil can hold more rainwater. Moreover, the Soil Conservation Service Runoff (SCS-CN) was used for predicting direct runoff from rainfall excess by calculating the overlying hydrologic soil group against the land use type (Jeong and Yoon, 2010).

Streams are also main factors in flooding, particular those in rural areas with dense rivers. Flood depth is strongly affected by closed streams and relative elevation (Galasso and Senarath, 2014).

2.2.2. Predictive model for flood depth created by multi-regression analysis

In order to derive a predictive model for flood depth, multi-regression analysis was performed using SPSS

software. The dependent variable was flood depth, and the independent variables were the environmental conditions that could affect flood occurrence. A flooded area map provided by the Water Resources Management Information System (WAMIS) was used to identify locations of flood occurrences. Of the areas mapped, 98 location points were derived, and environmental variables were created for characterizing the points.

Rainfall data during flood occurrences was provided by the Automatic Weather Station (AWS), and Inverse Distance Weighting (IDW) was applied to identify the precipitation at each flooded point. IDW is a spatial interpolation method with scattered observation points. Because it gives results with certain accuracy at the local level, this method is generally used for interpolation of precipitation (Hwang et al., 2010).

IDW interpolation function : $$u(x) = \frac{\sum_{k=0}^{N} W_k(x) u_k}{\sum_{k=0}^{N} W_k(x)}$$

u(x)= interpolated value
N= total number of known points used in interpolation
k= 1, 2, …, N
W= weighting value

Multi-regression analysis iteratively performed with different sets of independent variables for each pattern to determine the best model for predicting flood depth. After

comparing the R^2 , F, and significant P values of all models, an optimal model was selected for flood depth prediction.

2.2.3. Flood susceptibility determined by MaxEnt

MaxEnt, a model based on the statistical principle of logistic regression of entropy maximization, is used to derive the probability of a species occurrence with spatial distribution by detecting locations with similar characteristics as those of the species environment (Young et al., 2011; Convertino et al., 2013). In the MaxEnt model, the probability of occurrence is derived from logistic output, which transforms the model from exponential models.

The probability of class c given an input observation x :

$$P(c|x) = \frac{1}{Z}\exp(\sum_{i=0}^{N} w_{ci} \times f_i)$$

The normalization factor :

$$Z = \sum_{c' \epsilon C} \exp(\sum_{i=0}^{N} w_{c'i} \times f_i)$$

w×f= linear function (w: weights, f: feature value)

MaxEnt is used for predicting the occurrence of natural hazards because it essentially assumes that a certain event would occur under similar environmental conditions (Felicisimo et al., 2013; Vorpahl et al., 2012; Kim et al., 2013a; Kim et al., 2013b). In this study, MaxEnt was run with 390 flooded location points and environmental variables including 292 randomly selected points for training data and

98 for test data. Simulation with test data was for verification of the model. Moreover, correlation analysis between environmental variables was conducted by using SPSS to verify the existence of multicollinearity.

A pilot test was conducted to draw a reliable result by removing certain variables that reduce the accuracy of the model. The model was set to run 15 times iteratively and to draw the average probability map of flood occurrence. It showed the flood susceptibility from very low to very high by a standard deviation classification. A logistic threshold of 10 percentile training presence was used to divide insusceptible and susceptible areas.

The area under the receiver operating characteristic (ROC) curve (AUC) indicates the accuracy of the model. The AUC can be interpreted as the probability that the information of flood occurrence/ nonoccurrence is correctly divided by the optimal threshold (Subtil and Rabilloud, 2015). The nearer an AUC is to 1, the higher the accuracy of the model.

2.3. Flood risk assessment in 2050

The flood depth maps in 2050 were derived by applying precipitation under each RCP scenario of 2.6, 4.5, 6.0, 8.5 and the ensemble scenario to the multi-regression model. The average value and maximum value from the probability distribution of extreme rainfall were used to predict flood depth. The reclassified flood susceptibility map as a result of MaxEnt was superposed with flood depth maps for

representing the flood risk under the ensemble scenario.

Each class of flood susceptibility had a particular flood depth, from which the most vulnerable areas to flooding, which had high susceptibility and flood depth, were derived. Each flood depth was divided into three classes for interpreting the flood risk map including values greater than 0.3 m, 0.5 m, and 1.0 m. A built-up area is vulnerable when flooding is more than 0.3 m, and crop land can be damaged by floods of more than 0.5 m (National Emergency Management Agency, 2012). Moreover, in the case of floods greater than 1.0 m, the area should be protected or should be allowed to naturally dry (Shin et al., 2015).

In order to indicate the areas at high flood risk in 2050, the areas in which flood depth would be more than 1.0 m were selected for sample points. The possibility of high flood risk was derived by reflecting the flood depth map into MaxEnt as an environmental variable. In this process, the probability distribution of precipitation was considered by 10,000 iterations to indicate possibility of flood occurrence. The average and maximum possibility in 95% confidence were derived.

IV. Results and Discussion

1. Forecasting precipitation change under climate change

1.1. Probability distribution of rainfall in 2050 considering uncertainties

The probability distributions of daily precipitation and three-day accumulated precipitation of each RCP scenario are discussed in this section. All scenarios represented that days without rain accounted for the largest proportion in the 10-year study. In the case of daily precipitation, RCP 4.5 and 8.5 showed that the number of rainy days would increase and that the probability of extreme rainfall would be about twice that of RCP 2.6 and 6.0. In the case of accumulated precipitation, the probability of extreme rainfall would be about 1.85 higher times in RCP 4.5 and 8.5.

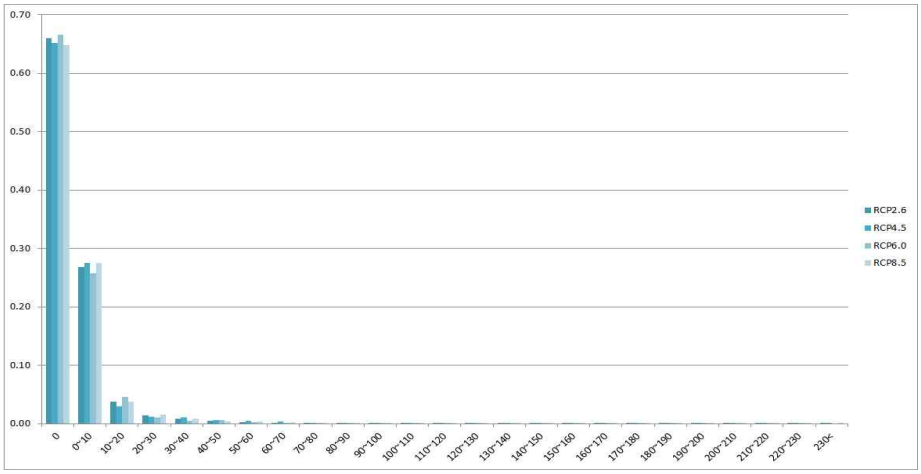

Fig. 11 The probability distribution of daily rainfall in each scenarios

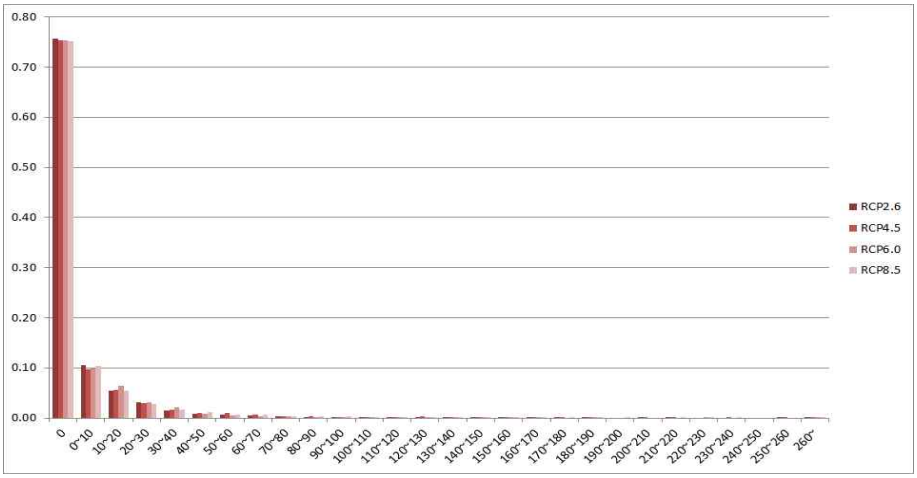

Fig. 12 The probability distribution of three-day accumulated rainfall

The Monte Carlo simulation for the scenario ensemble revealed that the average daily precipitation would be 2.60 mm and that the average accumulated precipitation would be 2.85 mm. However, the average values from extreme rainfall should be derived because they immediately affect flood depth. The probability distribution of extreme rainfall is thus given here. The average and maximum value of extreme rainfall would be increase in the case of both daily and accumulated precipitation. The maximum precipitation would increase as much as 106.76 mm and 55.66 mm in 2050 compared with current conditions, which implies that the maximum flood depth would be greatly increased, resulting in high flood risk.

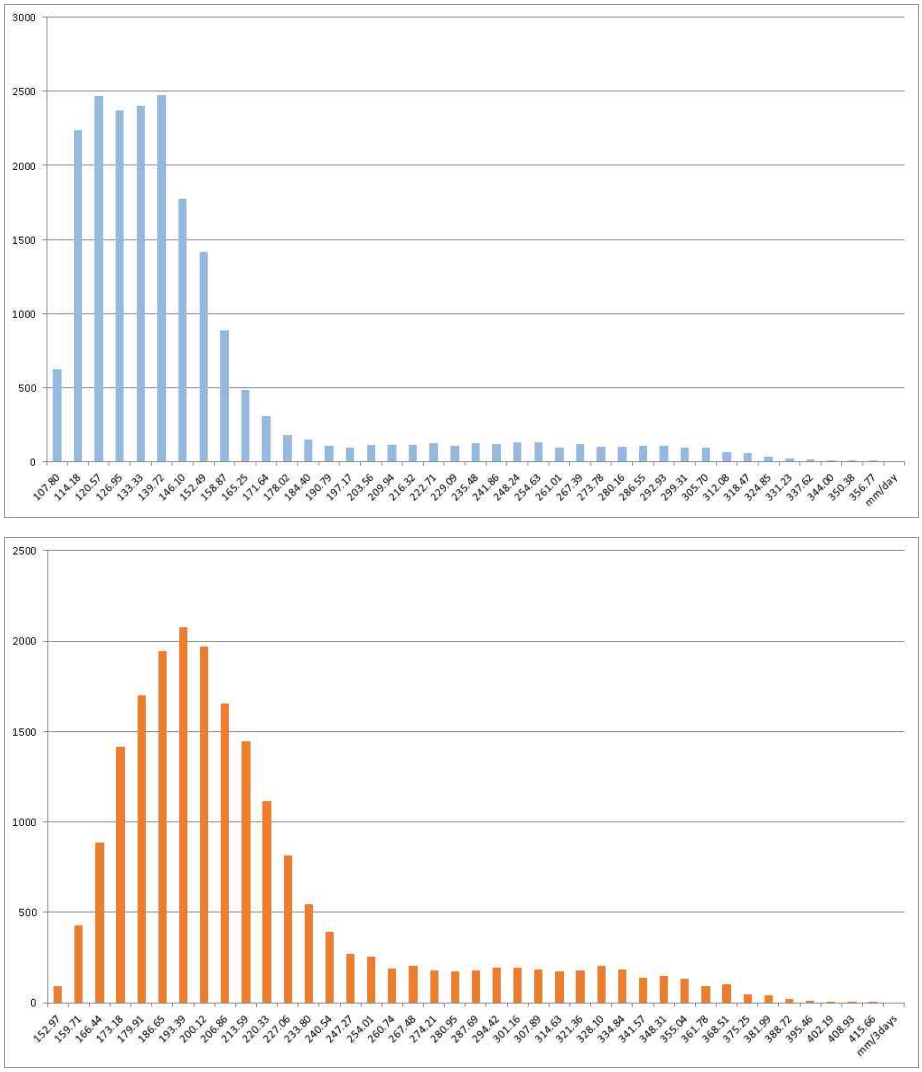

Fig. 13 The probability distribution of extreme daily rainfall (top) and extreme three-day accumulated rainfall (bottom)

Table 4 The pattern of extreme rainfall in current and future condition

		Minimum	Average	Maximum
2050 rainfall	daily precipitation (mm)	101.41	133.10	356.76
	accumulated precipitation (mm)	146.24	198.20	415.66
Current rainfall	daily precipitation (mm)	90.00	137.96	250.00
	accumulated precipitation (mm)	141.5	197.04	360

2. Flood risk assessment

2.1. Predictive model for flood depth

In the multi-regression analysis, seven variables with statistical significance were selected: daily precipitation, three-day accumulated precipitation, elevation, distance to stream, elevation of the nearest stream, relative elevation to the nearest stream, and TPI.

Both daily precipitation and accumulated precipitation had high correlation with flood depth; however, they also showed high correlation with each other. For this reason, the flood depth model was divided into two models, which included daily precipitation and accumulated precipitation, respectively. Moreover, the flood depth-precipitation curve showed that both linear and quadratic relationships could be delineated from the scatter plots. Thus, the multi-regression was conducted in the cases of both relationships.

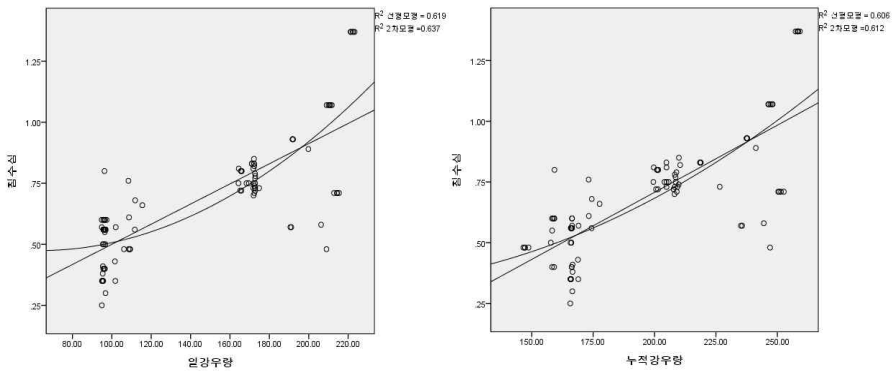

Fig. 14 The scatter plots: daily precipitation and flood depth (left), three-day accumulated precipitation and flood depth (right)

The best multi-regression model was selected among 16 models resulting from different sets of significant variables with the criteria of high R^2 , F and P values of regression coefficients. Moreover, the model was checked for multicollinearity, homoscedasticity, and normality of residuals. From this process, a regression equation was derived to predict flood depth. The independent variables were selected: include daily precipitation with a linear relationship, X_{daily}; three-day accumulated precipitation with linear relationship, X_{accum}; relative elevation to the nearest stream, X_{stream}; and TPI, X_{tpi}.

$$Flood\ depth = 0.101 + 0.003 X_{daily} - 0.032 X_{stream} - 0.017 X_{tpi} \quad \cdots\cdots \text{Eq.(1)}$$

$$Flood\ depth = -0.241 + 0.004 X_{accum} - 0.030 X_{stream} - 0.019 X_{tpi} \quad \cdots\cdots \text{Eq.(2)}$$

Equation (1) is used when daily precipitation was considered as a main factor representing rainfall effects. Equation (2) considers three-day accumulated precipitation.

Both of the models meet the hypothesis of regression analysis and have the highest R^2 value.

Table 5 The models for flood depth prediction
(Eq.(1): R^2 =.738, F=88.323, Eq.(2): R^2 =.729, F=84.097)

Eq.(1)	Coefficient	Standardized Coefficient	t	Significant	Tolerance	VIF
(Constant)	0.101		2.336	0.022		
X_{daily}	0.003	0.582	8.836	0.000	0.643	1.556
X_{stream}	−0.032	−0.240	−4.474	0.000	0.965	1.036
X_{tpi}	−0.017	−0.282	−4.271	0.000	0.638	1.567
Eq.(2)	Coefficient	Standardized Coefficient	t	Significant	Tolerance	VIF
(Constant)	−0.241		−2.956	0.004		
X_{accum}	0.004	0.559	8.486	0.000	0.666	1.501
X_{stream}	−0.030	−0.220	−4.012	0.000	0.958	1.044
X_{tpi}	−0.019	−0.313	−4.767	0.000	0.669	1.494

2.2. Flood susceptibility

Before performing MaxEnt, correlation analysis between environmental variables was conducted by using SPSS. The results showed that correlation between elevation, slope, and VRM was very high with values of 0.802 between elevation and slope, 0.771 between elevation and VRM, and 0.698 between elevation and VRM. In order to select the variables to be removed among them, a pilot test was conducted by

using MaxEnt. The results indicated that elevation had the highest contribution to the model; therefore, slope and VRM were removed.

Moreover, TWI was removed from the independent variables because it included numerous NoData values. As previously mentioned, deeper soil generally reduce flooding; however, the opposite result was derived with this model. After the pilot test was conducted, the following environmental variables were selected in order to improve the accuracy of the model: elevation, plan curvature, profile curvature, soil drainage, runoff curve number, and distance to stream.

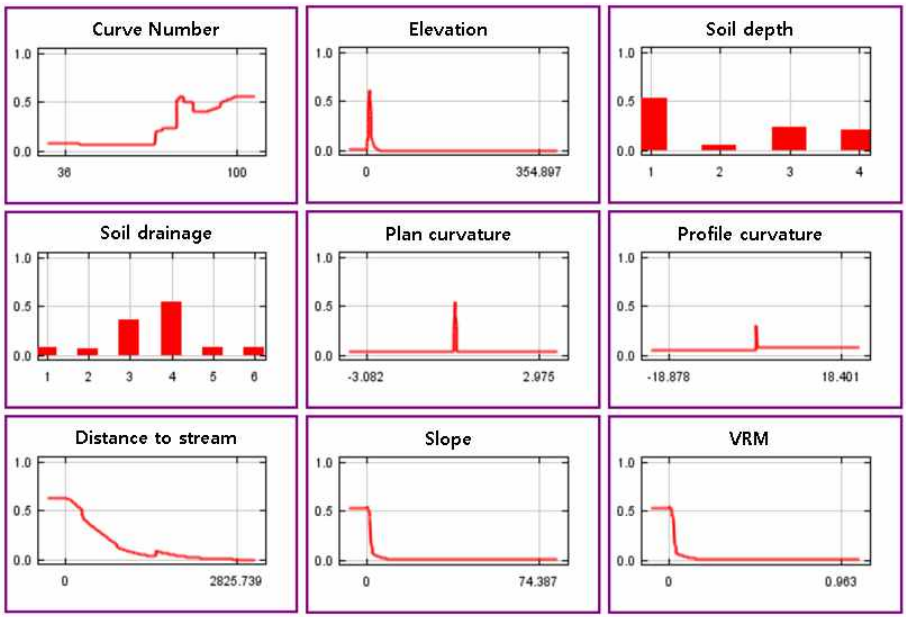

Fig. 15 The response curves of each environmental variables on flood susceptibility prediction

The AUC showed that the output of the model was available. The ROC curves with training data (red line) and test data (blue line) almost overlapped and showed high AUC, indicating that the model has good fit and predictive power. The 15 iterations revealed an average AUC of 0.858, which is quite high.

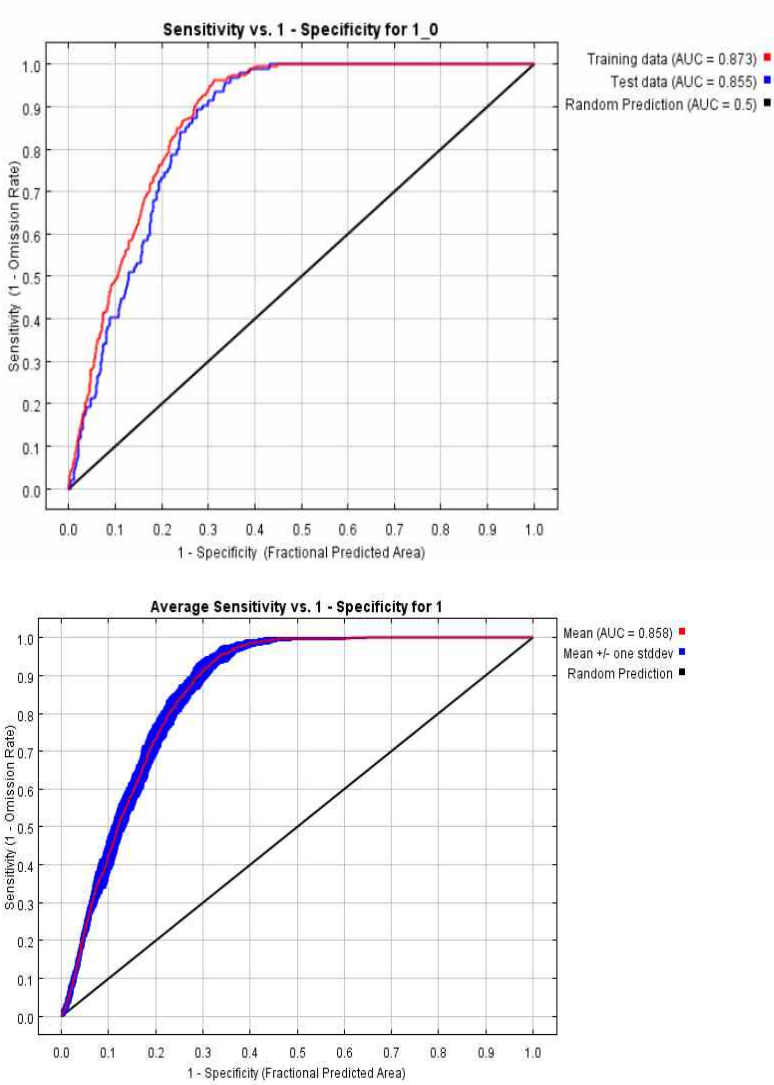

Fig. 16 The ROC curve and Area Under the Curve (AUC)

For the flood susceptibility map in Gimpo, the 10 percentile training presence (= 0.36) was used as a logistic threshold defining susceptible areas. By using this threshold, susceptible areas were selected to include 90% of the flood location data used to develop MaxEnt. Areas with a probability of flood occurrence greater than 0.36 were defined as susceptible areas. As a result of reclassification, classes 5, 6, 7, and 8 were designated as areas requiring special management for safety in Gimpo.

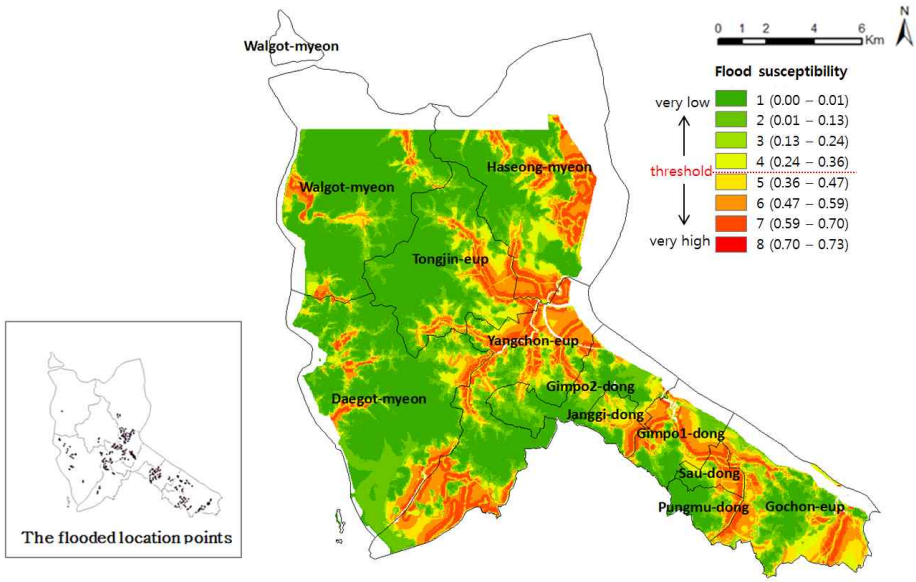

Fig. 17 The map of flood susceptibility

The areas of classes 5 to 8 representing flood susceptible areas accounted for 28% of the area in Gimpo. Areas of class 8, with very high susceptibility, were rare at 0.007%; however, those of class 7, with high susceptibility, accounted for 7% of the entire area.

In Haseong-myeon, 37% of the area showed flood possibility even though floods had not occurred there previously, which indicates that environmental conditions of the area are similar to those of flooded locations.

Fig. 18 The flooded areas derived from MaxEnt in Haseong-myeon (left) and the areas prone to floods in Walgot-myeon (right)

The discrepancy between actual conditions and model prediction for Haseong-myeon was detected by field survey. Although this area has the same vulnerability to floods as other areas with similar environmental conditions, crop land runoff in Haseong-myeon is held by an adjacent the stream. Crop lands flooded by stream overflow have not been recorded as flooded areas. Therefore, Haseong was excluded from the flooded area map even though its environmental conditions are similar to those of flooded areas.

Yangchon, Gimpo1, and Sau were determined to be vulnerable to floods because their susceptible areas accounted for more than 50% of each district's area, and their highly susceptible areas were 16.06%, 12.02%, and 17.21%, respectively. Gochon, designated as class 8, was the most susceptible among the districts. These districts have actually been reported as flood prone during a five-year

period of 2006-2010 (Choi et al., 2012).

On the contrary, Walgot, Gimpo 2, and Pungmu would be safer than other districts because more than 80% of these regions do not show susceptibility to floods. Gimpo2 is the site of Gimpo Han-gang New Town, which is scheduled for construction during the next five years. Only 1% of the area in Gimpo 2 was designated as susceptible; therefore, the location of the new town is determined to be safe against flooding.

Table 6 The flood susceptibility of each administrative districts

Administrative districts	Insusceptible (%)	class 5	class 6	class 7	class 8
		moderate susceptible ←——→ very susceptible			
Walgot	89.98	3.68	4.05	2.29	-
Daegot	86.87	4.15	5.74	3.23	0.002
Haseong	62.99	9.30	14.38	13.33	-
Tongjin	78.61	7.59	8.54	5.26	-
Yangchon	49.83	11.18	22.93	16.06	0.002
Gimpo 1	48.64	14.95	24.39	12.02	-
Gimpo 2	84.71	8.21	5.61	1.47	-
Janggi	60.57	18.38	14.57	6.48	-
Sau	42.50	12.86	27.43	17.21	-
Pungmu	80.62	6.55	7.94	4.89	-
Gochon	55.87	17.20	18.29	8.57	0.07

2.3. 2050 flood depth under climate change

The RCP 4.5 scenario for predicted flood depth in 2050 showed the highest vulnerability to flood depth. These conditions include flood depth of 3.91 m under the maximum precipitation of extreme rainfall; the flood depth is less than 2 m under the other three scenarios. On average, the flood depth would be 1.73-1.78 m under daily precipitation and 1.98-2.05 m under the three-day accumulated precipitation. The accumulated precipitation would cause a more severe flood depth than the daily precipitation both average and maximum flood depth.

Table 7 The predicted flood depth under each RCP scenarios

Extreme rainfall event in 2050		Maximum flood depth in Gimpo (m)			
		RCP 2.6	RCP 4.5	RCP 6.0	RCP 8.5
Daily precipitation	average	1.78	1.76	1.77	1.73
	maximum	1.96	3.91	1.88	1.93
3 day accumulated precipitation	average	1.98	2.05	1.98	2.05
	maximum	2.25	4.69	2.42	2.36

Flood depth can be used to plan adaptive land use. However, because each scenario has a different range of the values, determination of the most probable case is complex. For a decision-maker in land use planning, it is important to integrate the results of future prediction such that each

scenario is drawn into one interpretable scenario considering uncertainties. For this reason, the ensemble with four RCP scenarios was performed to determine the flood depth from the ensemble scenario.

The flood depth caused by daily precipitation of extreme rainfall would be 0.01-0.05 m at the safest area, and 1.64-2.34 m at the most vulnerable area, with average depths of 0.04 m and 1.73 m, respectively. In the case of accumulated precipitation of extreme rainfall, the flood depths would be 0.01-0.06 m and 1.82-2.89 m at the safest area and the most vulnerable areas with average depths of 0.03 m and 2.02 m, respectively.

A comparison of the flood depth resulting from daily precipitation and accumulated precipitation revealed that the flood depth was much higher in the latter case. This result implies that the three-day accumulated precipitation has a greater contribution to floods than daily precipitation. Therefore, it is necessary to define the effects of accumulated precipitation for adapting to floods.

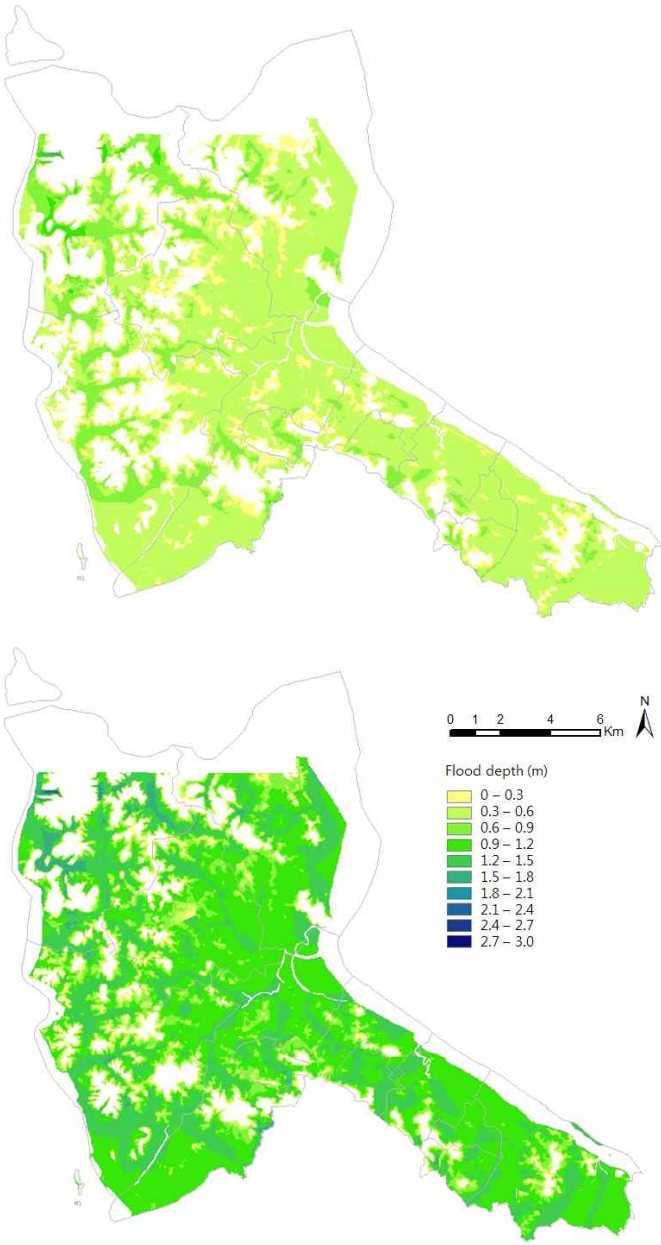

Fig. 19 Flood depth in the daily precipitation (pcp.)
(top: average pcp.= 133.10 mm, bottom: maximum pcp.= 356.76 mm)

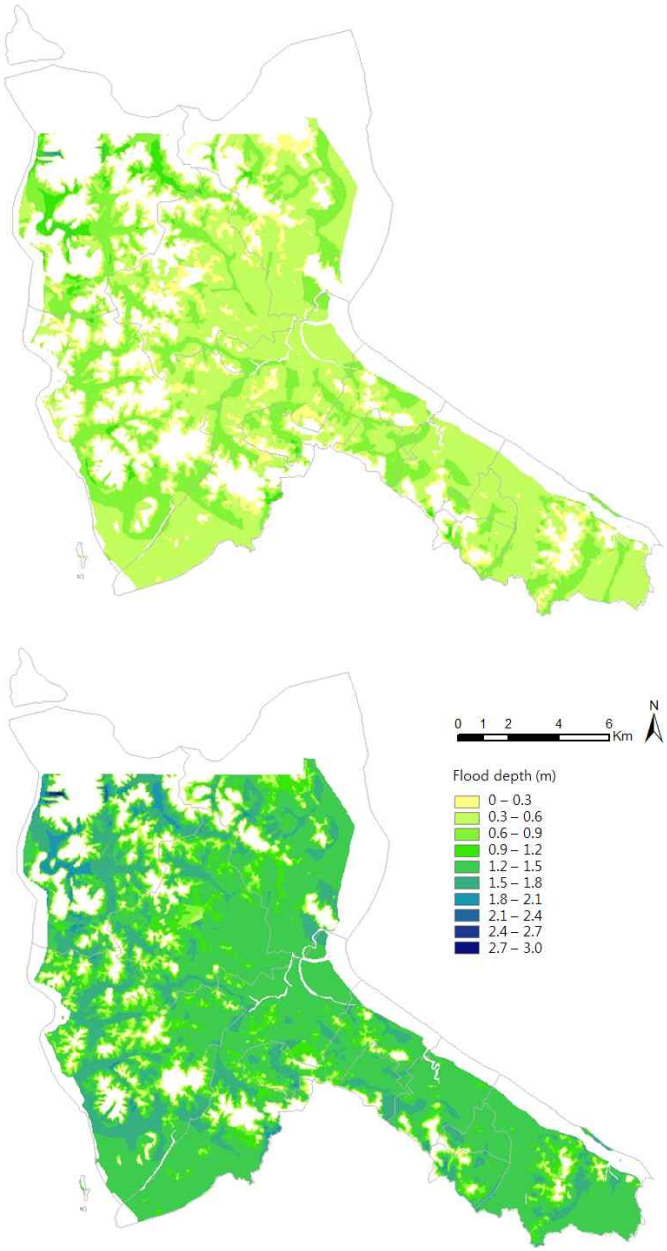

Fig. 20 Flood depth in the 3 day accumulated precipitation (pcp.)
(top: average pcp.= 198.20 mm, bottom: maximum pcp.= 415.66 mm)

2.4. 2050 flood risk map from flood depth and susceptibility

The flood risk map shows the flood depth at each class of flood susceptibility from class 5 representing moderately susceptible areas to class 8 representing very susceptible areas. At the areas of class 8, the maximum flood depths caused by daily and accumulated precipitation would be 1.36 m and 1.63 m, respectively. Although these areas have the highest flood risk in 2050, they account for less 0.01% of Gimpo.

For class 7, most of areas at risk of flooding would be located near streams. This result corresponds with previous research showing that flood depth has a strong relationship with the distance to a river (Galasso and Senarath, 2014). In the case of average daily precipitation, 17.26km² would have a flood depth of more than 0.3 m, which indicates the vulnerable areas requiring land buildup. In addition, 7,200 m² show flooding of more than 1.0 m. In the case of average accumulated precipitation, the areas with flood depth greater than 1.0 m would increase by 139,500 m². Therefore, construction should be prohibited in these areas.

Class 5 areas show lower flood risk compared with other classes. The maximum flood depths caused by daily and accumulated precipitation would be 1.78 m and 2.09 m, respectively. Although flood depths are extremely high, the flood risk would be not high when considering flood susceptibility. Therefore, planners could apply strategies for

adaptation and allocation of the land use in these areas.

For example, when a strong adaptive policy is created, areas of class 5 would be regarded as risky areas. However, when a limited policy is created against flooding, areas with the highest risk, such as class 8 with flood depth greater than 1.0 m, would be restricted.

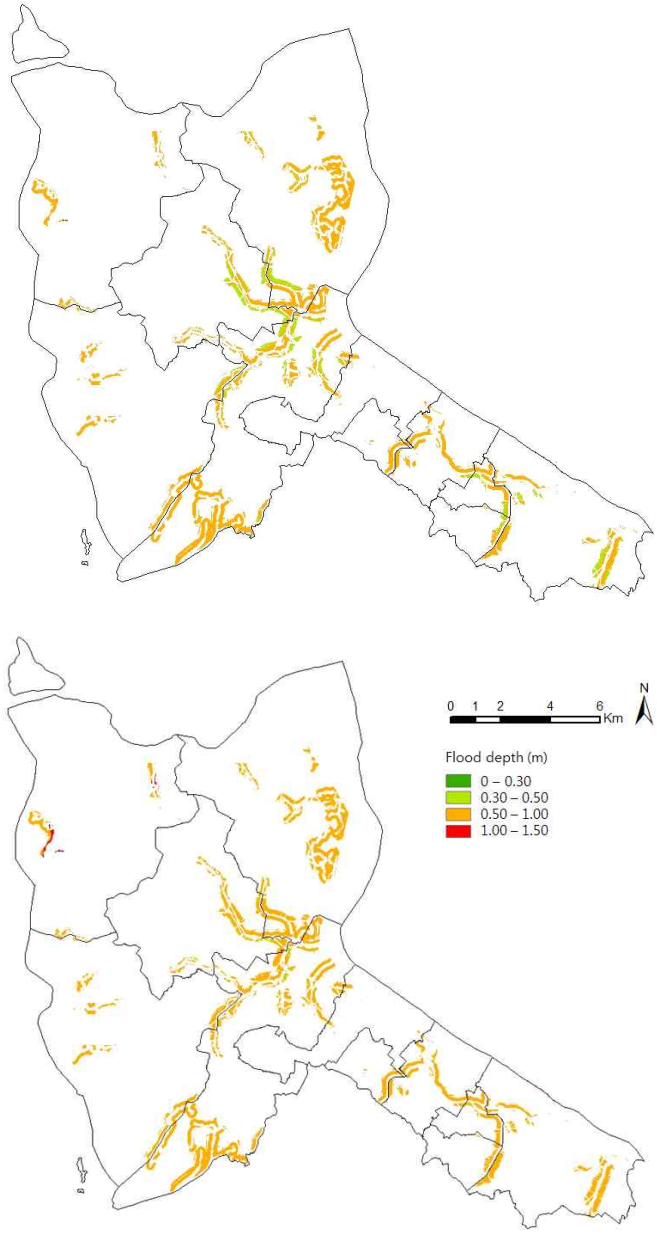

Fig. 21 Flood depths at class 7 of flood susceptibility in average of extreme daily pcp. (top) and accumulated pcp. (bottom)

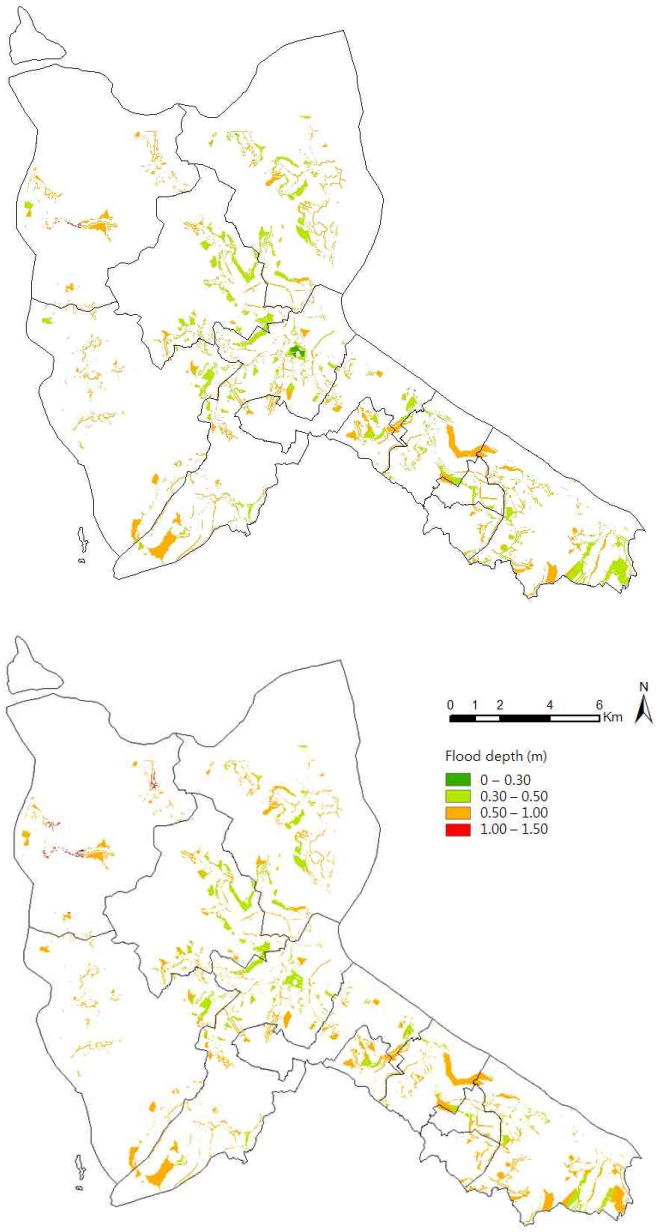

Fig. 22 Flood depths at class 5 of flood susceptibility in average of extreme daily pcp. (top) and accumulated pcp. (bottom)

The high flood risk map reflecting flood depths of 2050 showed a range of uncertainties in flood depth possibility of more than 1.0 m. The standard deviation showed the uncertainty of high flood risk considering probability distribution of flood depth in 2050. The susceptible areas (colored red in Fig. 23) would have a wide range of uncertainty as precipitation changes.

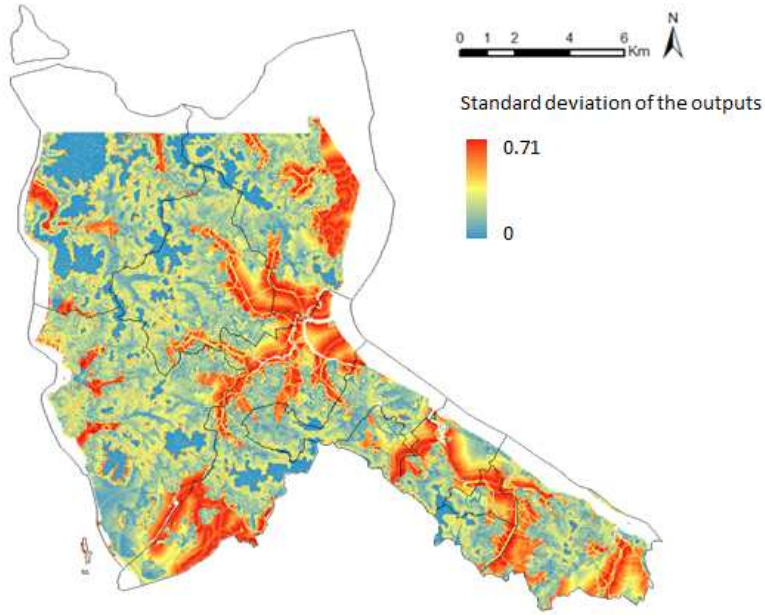

Fig. 23 The standard deviation of high risk possibility maps in 2050

The highest possibility from the flood risk map considering current flood depth would be 0.73, although the value would increase to 0.96 for 2050. Compared with current possibilities, the areas with low possibility of less than 0.2 would be reduced as much as 12.93 km^2 (minimum possibility) to 109.32 km^2 (maximum possibility). On the

other hand, areas with possibilities over 0.2 would increase in 2050.

On average, Gimpo would include 42.38 km^2 of areas where flood depth would be over 1.0 m (possibility$\geq$0.5). Yangchon would include the largest areas: 12.72 km^2 of flooded areas would have at least 1.0 m of flood depth. As the map of maximum possibility in 95% confidence, it would be possible that 38.54 % of non-flood areas turn to flood zone in 2050.

Table 8 The change of areas at each possibility on high flood risk

Possibility at high risk	The areas in the present (%)	The areas in 2050 (%)	
		Minimum	Maximum
0 - 0.1	57.96	51.68	10.51
0.1 - 0.2	6.27	6.75	4.72
0.2 - 0.3	4.71	6.97	23.12
0.3 - 0.4	5.67	7.47	21.93
0.4 - 0.5	8.06	8.50	15.44
0.5 - 0.6	11.84	8.84	15.15
0.6 - 0.7	5.48	9.70	7.79
0.7 - 0.8	0.00	0.07	1.21
0.8 - 0.9	·	0.02	0.13
0.9 - 1.0	·	0.00	0.00

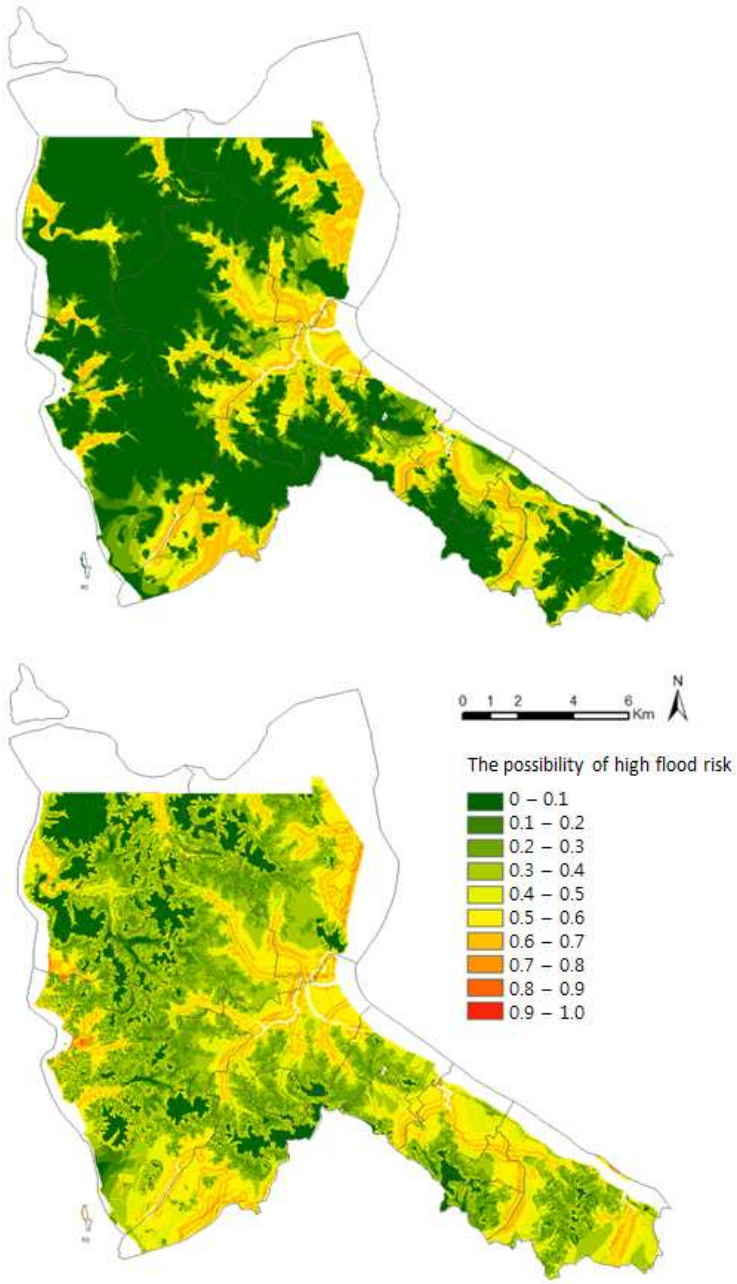

Fig. 24 The possibility of high flood risk (flood depth≥1.0 m) in 2050: Average (top) and maximum possibility in 95% confidence (bottom)

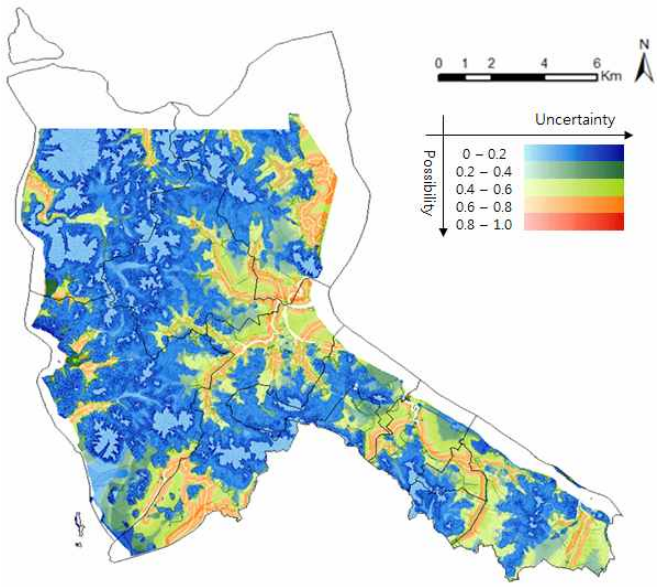

Fig. 25 The matrix of possibility on high risk and its uncertainty in 2050

The matrix of possibility on high flood risk and uncertainty indicated that the most risky areas, with high possibility and low uncertainty (colored light red in Fig. 25) would be located in Walgot-myeon covering 5,400 m^2. On the contrary, Daegot-myeon would include the areas with low possibility in a wide range of uncertainty (colored dark blue in Fig. 25). These areas have been used as crop lands, however, they have the potential of being developed as built up lands when considering safer land use planning.

3. Application for spatial planning

Recently, an adaptation strategy related to spatial planning has been implemented to improve the resilience of cities and to reduce the risk under climate change (UN-HABITAT, 2009; Brown, 2011). Countries advanced in disaster prevention measures such as the United Kingdom and Japan have applied these adaptation strategies in city planning. In European countries vulnerable to sea level rise, adaptation to flood risk has been considered in planning land use and determining the location of development areas. South Korea has also shown progress in employing similar projects on vulnerability assessment and applying the outcome to spatial planning (Korea Research Institute of Human Settlement, 2009; Ministry of Land, Infrastructure and Transport, 2011).

The flood risk map developed in this study can be used for land use planning in the future. Gimpo has been announced as the site of a master development plan by 2020. Among the areas planned for development, the Hakun 3-4 industrial complex would incur flooding of 0.3-0.5 m once per year and 0.5-1.0 m once every two years. It is located in classes 6 and 7 of flood susceptibility; thus the flood risk is high. Moreover, the industrial complex is affected by the effects of climate change (Choi et al., 2009); therefore, disaster prevention systems should be installed in this area.

The most effective prevention measure is to spatially distribute the land considering flood risk rather than the

developed areas at the city planning phase. It would be not be practical to expand a drainage system as much as necessary or to change land cover to a permeable surface in developed areas. Therefore, it is necessary to select areas not previously developed, such as Gimpo, for flood prevention.

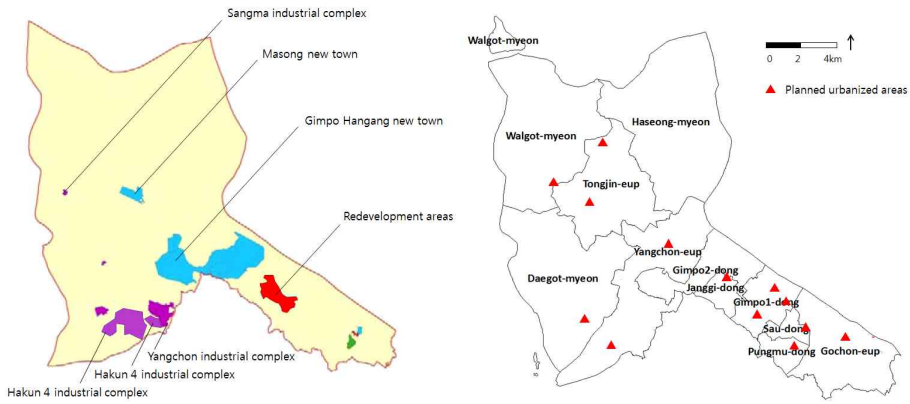

Fig. 26 Maps of current development areas (left) and planned urbanized areas (right)

Under the master plan in Gimpo by 2020, as much as 27.60 km^2 is considered as development potential. These locations are probable and do not include obvious development boundaries; thus, negative development could be performed in the areas of high flood risk.

The local government has provided a map of development areas showing developed, developable, and undevelopable lands. However, the developable lands include areas at risk of flooding under climate change. Therefore, there areas should be changed to undevelopable lands in the next spatial planning project in Gimpo.

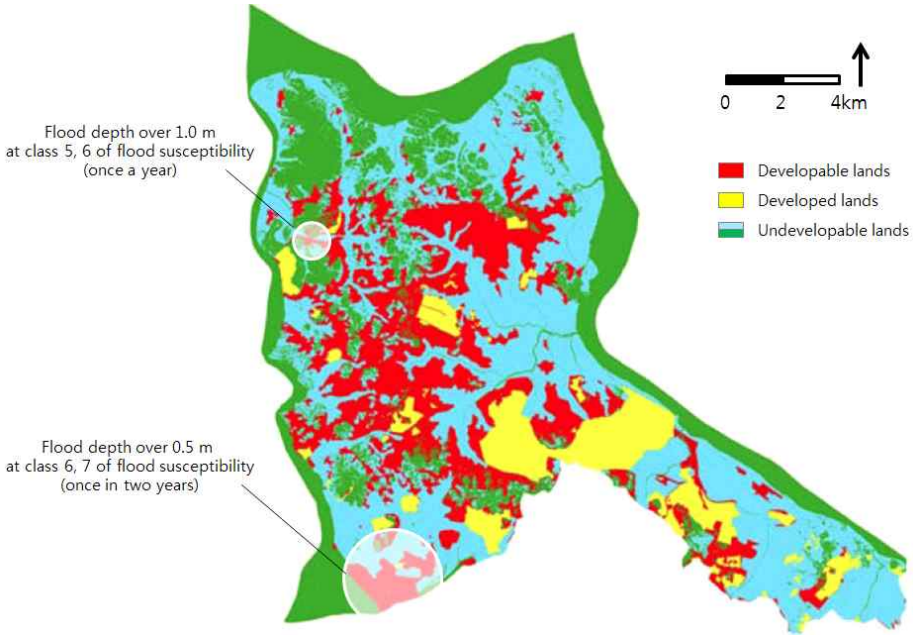

Fig. 27 A map of development areas of Gimpo (Gimpo, 2007)

V. Conclusion

An ensemble of RCP scenarios was performed by Monte Carlo simulation in order to consider uncertainties in climate change scenarios, and the results will be used for flood risk assessment in 2050 in Gimpo. By using a predictive model for flood depth established in this study and the flood susceptibility map, areas at risk of flooding were determined. The results of the risk map can be used to support plans of adaptive cities against flooding under climate change.

The extreme rainfall would intensify in 2050 compared with current conditions; therefore, strategies for adaptation should be employed. In development areas that are vulnerable to floods, the flood risk should be identified and addressed for future land use planning in Gimpo.

Changes in precipitation and environmental variables were considered in the flood risk assessment; however, inclusion of adaptive infrastructures such as drainage systems was limited. This study could be improved with more accurate and available data from field survey. Moreover, prior probability of rainfall, which causes changes in soil water-holding capacity, was out of the scope of this study because the ensemble scenario was used. This variable could be reflected in predicting flood risk under each scenario in future study.

This study is significant because flood risk was assessed with probability distribution of rainfall events under various

scenarios to quantitatively provide a range of uncertainties. The results can support land use planners in establishing decision-making criteria and reasonable planning. In addition, the model for predicting flood depth can be more easily used by planners than a complex hydrological model.

The new paradigm of land use planning under climate change is defined as reducing impacts and adapting to natural hazards in cities. Therefore, risk assessment is needed at the beginning of land use planning. This study can be used as basic research to determine the locations of adaptation strategy implementation such as green spaces and prevention systems in addition to land use allocation.

VI. Reference

■ Foreign articles

Allen M., Stott P., Mitchell J., Schnur R., Delworth T., 2000. Quantifying the uncertainty in forecasts of anthropogenic climate change, Nature, 407: 617-620.

Australia, 2009. Climate Change Risk Assessment: Adaption Report, Cooma Monaro Shire Council.

Donald B., 2011. Making the linkages between climate change adaptation and spatial planning in Malawi, Environmental science & policy, 14(8): 940-949.

Convertino M., Troccoli A., Catani F., 2013. Detecting fingerprints of landslide drivers: A MaxEnt model, Journal of Geophysical Research: Earth Surface, 118: 1367-1386.

Cvetko R., Chase K.W., Magleby S.P., 1998. New metrics for evaluating monte carlo tolerance analysis of assemblies, Proceeding of the ASME international mechanical engineering conference and exposition, Anaheim, CA, 15-20.

Diallo I., Sylla M.B., Giorgi F., Gaye A.T., Camara M., 2012. Multimodel GCM-RCM ensemble-based projections of temperature and precipitation over West Africa for the early 21st centry, International Journal of Geophysics, 2012: 1-19.

Du, J., 2007. Uncertainty and ensemble forecast, Science and technology infusion climate bulletin, NOAA' s national weather service office of science and technology.

Fedeski M. and Gwilliam J., 2007. Urban sustainability in the presence of flood and geological hazards: The development of a GIS-based vulnerability and risk assessment methodology, Landscape and Urban Planning, 83: 50-61.

Felicisimo A., Cuartero A., Remondo J. and Quiros E., 2013. Mapping landslide susceptibility with logistic regression, multiple adaptive regression splines, classification and regression trees, and maximum entropy methods: a comparative study, Landslides, 10: 175-189.

FEMA, 2014. Guidance for Flood Risk Analysis and Mapping: Flood Depth and Analysis Grids, Guidance Document 14.

Foudi S., Oses-Eraso N., Tamayo I., 2015. Integrated spatial flood risk assessment: The case of Zaragoza, Land Use Policy, 42: 278-292.

Galasso C., Senarath S., 2014. A Statistical Model for Flood Depth Estimation in Southeast Europe, Vulnerability, Uncertainty, and Risk, ASCE 2014, 1415-1424.

Huong H.T.L. and Pathirana A., 2012. Urbanization and climate change impacts on future urban flooding in Can Tho city, Vietnam, Hydrol. Earth Syst. Sci., 17: 379-394.

Hydrologic engineering center, 2010. HEC-RAS river analysis system, user' s manual version 4.1.

IPCC, 2000. IPCC Special Report: Emissions Scenarions A special report of IPCC working group Ⅲ, Cambridge University Press.

IPCC, 2013. Climate Change 2013: The Physical Science Basis. Contribution of Working Group I to the Fifth Assessment Report of the Intergovernmental Panel on Climate Change, Cambridge University Press, Cambridge, United Kingdom and New York, NY, USA.

Jenness J., 2006. Topography Position Index TPI Landform Slope Classification Standardization Neighborhood Statistics, Topographic Position Index (TPI) v. 1.2 extension guidance.

Knutti R., Sedlacek J., 2013. Robustness and uncertainties in the new CMIP5 climate model projection, Nature climate change, 3: 369-373.

Leutbecher M., Palmer T.N., 2008. Ensemble forecasting, Journal of computational physics, 227: 3515-3539.

Mendes D., Marengo J., 2010. Temporal downscaling: a comparison between artificial neural network and autocorrelation techniques over the Amazon Basin in present and future climate change scenarios, Theor Appl Climartol, 100: 413-412.

Moel H., Bouwer L., Aerts J., 2014. Uncertainty and sensitivity of flood risk calculations for a dike ring in the south of the Netherlands, Science of the total environment, 473-474: 224-234.

Netherlands, 2005. Flood risks and safety in the Netherlands, FLORIS study full report.

New M., Hulme M., 2000. Representing uncertainty in climate change scenarios: a Monte-Carlo approach, Integrated Assessment, 1: 203-213.

Norway, 2011. Preliminary flood risk assessment in Norway, report.

Nusret D., Dug S., 2012. Applying the inverse distance weighting and kriging methods of the spatial interpolation on the mapping the annual precipitation in Bosnia and Herzegovina, International Congress on Environmental Modelling and Software Managing Resources of a Limited Planet, Sixth Biennial Meeting, Leipzig, Germany.

Pourali S. H., Arrowsmith C., Chrisman N., Matkan A. A., Mitchell D., 2014. Topography Wetness Index Application in Flood-Risk-Based Land Use Planning, Applied Spatial Analysis and Policy, 1-16.

Queensland, 2011. Climate change risk management matrix: a process for assessing impacts, adaptation, risk and vulnerability, Department of Environment and Resource Management.

Randall D.A., R.A. Wood, S. Bony, R. Colman, T. Fichefet, J. Fyfe, V. Kattsov, A. Pitman, J. Shukla, J. Srinivasan, R.J. Stouffer, A. Sumi and K.E. Taylor, 2007. Cilmate Models and Their Evaluation. In: Climate Change 2007:

The Physical Science Basis. Contribution of Working Group I to the Fourth Assessment Report of the Intergovernmental Panel on Climate Change [Solomon, S., D. Qin, M. Manning, Z. Chen, M. Marquis, K.B. Averyt, M.Tignor and H.L. Miller (eds.)]. Cambridge University Press, Cambridge, United Kingdom and New York, NY, USA.

Rauscher S., Giorgi F., Diffenbaugh N., Seth A., 2008. Extension and intensification of the Meso-American mid-summer drought in the twenty-first century, Climate dynamics, 31(5): 551-571.

Richardson J. L., Arndt J. L., Montgomery J. A., 2001. Hydrology of wetland and related soils, Wetland soils: genesis, hydrology, landscapes and classification, CTC Press, USA, 35-50.

Sappington J., Longshore K., Thompson D., 2007. Quantifying Landscape Ruggedness for Animal Habitat Analysis: A Case Study Using Bighorn Sheep in the Mojave Desert, The Journal of Wildlife Management, 71(5): 1419-1426.

Storch H., Downes N., Katzschner L., Thinh N., 2011. Building resilience to climate change through adaptive land use planning in Ho Chi Minh city, Vietnam, Local sustainability, 1: 349-363.

Subtil F., Rabilloud M., 2015. An enhancement of ROC curves made them clinically relevant for diagnostic-test comparison and optimal-threshold determination, Journal

of Clinical Epidemiology, Article in Press.

Tebaldi C., Knutti R., 2007. The use of the multi-model ensemble in probabilistic climate projections, Phil. Trans. R. Soc. A, 365: 2053-2075.

Tebaldi C., Smith R., Nychka D., Mearns L., 2005. Quantifying uncertainty in projections of regional climate change: A bayesian approach to the analysis of multimodel ensembles, Journal of climate, 13: 1524-1540.

U.K., 2006. Development and flood risk, report.

UN-HABITAT, 2009. Global Reports on Human Settlements; Planning Sustainable Cities. Earthscan Publication, London.

US, 2014. The flood hazard mapping: Flood risk project life cycle, FEMA homepage, www.fema.gov/risk-map-flood-risk-project-lifecycle, Uploaded at 10/06/2014,

Vorpahl P., Helmut E., Michael M. and Boris S., 2012. How can statistical models help to determine driving factors of landslides?, Ecological Modelling, 239: 27-39.

Walker W.E., Harremoes P., Rotmans J., Sluijs J.P., Asselt M.B.A., Janssen P., Krayer von Krauss M.P., 2003. Defining uncertainty: A conceptual basis for uncertainty management in model-based decision support, Integrated Assessment, 4(1): 5-17.

Wilby R.L., Harris I., 2006. A framework for assessing uncertainties in climate change impacts: Low-flow

scenarios for the River Thames, UK, Water resources research, 42: 1-10.

Young N., Carter L., Evangelista P. A., 2011. A MaxEnt Model v3.3.3e Tutorial (ArcGIS v.10), Colorado, USA: Natural Resource Ecology Laboratory at Colorado State University and the National Institute of Invasive Species Science.

■ Articles in Korean

Choi K., Jang H., Lim E., Moon S., Kang Y., 2009. The study for Development of Industrial Climate Change Adaptation Strategy -Mainly focused on the Seaside industrial complex-, The Korean Journal of LCA, 10(1): 63-72.

Gimpo, 2007. Urban planning in Gimpo, 2020.

Hwang Y., Jung Y., Lim K., Heo J., 2010. Comparison of Daily Rainfall Interpolation Techniques and Development of Two Step Technique for Rainfall-Runoff Modeling, Journal of Hydeo-environment Research, 43(12): 1083-1091.

Jeong J., Yoon Y., 2010. Practical planning on water resource version 2, Goomiseogwan.

Joo J., Yang J., Kim J., 2013. Assessment of Inundation Risk Degree for Urban Areas, Journal of the Korean Society of Hazard Mitigation, 13(1): 129-136.

Kang S., Jung J., 2012. Study on the distribution characteristics

of storm damage area: the case of Gyeonggi-do, Journal of Korean Planners Association, 32(5): 507-517.

Kim H., Lee D., Mo Y., Kil S., Park C., Lee S., 2013a. Prediction of Landslides Occurrence Probability under Climate Change using MaxEnt Model, Journal of environmental impact assessment, 22(1): 39-50.

Kim H., Lee D., Park C., 2013b. A Study on Selection for Vulnerable Area of Urban Flooding Adaptable Capacity Using MaxEnt in Seoul, Journal of Korea Planners Association, 48(4): 205-217.

Kim J., Cho H., Cho Y., 2014. Projection of Climate Change with Uncertainties: 2. Internal Variability, Journal of Korean Society of Hazard Mitigation, 14(5): 329-339.

Korea Meteorological Administration, 2012. A report on forecasting climate change in the Korean Peninsula.

Korea research institute of human settlement, 2005. Analysis of flood damage characteristics and development of flood damage index.

Korea research institute of human settlement, 2009. Research on safer urban planning under climate change (I).

Lee D., Kim J., Jung H., 2006. A Comparative Study on General Circulation Model and Regional Climate Model for Impact Assessment of Climate Changes, The Journal of environmental impact assessment, 15(4): 249-258.

Lee H., Noh S., 2012. Analytics of high-end statistics: theory and practice, Bupmoonsa.

Lee J., Lee J., 2004. Financial Engineering using Excel/VBA, Gyeongmunsa.

Ministry of Environment, 2011. Guideline for simulation of drainage systems against floods.

Ministry of Land, Infrastructure and Transport, 2011, 2013. The revised plan of urban general planning.

Nam S., 2011. Geomorphic Characteristics of Hill Wetlands in Sungnam Region, Journal of geography, 57:1-19.

National Emergency Management Agency, 2012. A guideline for creating hazard maps.

National Institute of Environmental Research, 2012. Base study of model development for climate friendly and safe society in 2050, The final report.

Park M., Song Y., Kim S., Park M., 2012. A Study on the Assessment Method for High-risk Urban Inundation Area Using Flood Vulnerability Index., The Journal of Korean Society of Hazard Mitigation, 12(2): 245-253.

Seo Y., 2011. Risk Analysis in Water Resources Planning: Flood Risk Analysis with Consideration of Rainfall Uncertainty, Dissertation of degree of doctor.

Shin S., Park C., Son E., 2015. alyzing the Effects and Costs of Flood Protection Measures for Buildings, The Journal of Korean Planners Association, 50(2): 243-260.

Song W., Kim E., 2012. A Comparison of Machine Learning Species Distribution Methods for Habitat Analysis of the Korea Water Deer (Hydropotes inermis argyropus), The

Korean Journal of Remote Sensing, 28(1): 171-180.

The Seoul Institute, 2011. Research on relationship between land use characteristics and flooded areas.

VII. Appendix

Table 1 Correlation coefficient of all variables (N=98) (* Correlation is significant at the 0.01 level (2-tailed).)

		flood depth	daily rainfall	3 day rainfall	distance to stream	elevation	slope	plan curvature	profile curvature	elevation of stream	relative elevation	TPI	TWI	VRM
flood depth	Pearson P value	1	.787* .000	.779* .000	.453* .000	.516* .000	−.017 .868	−.087 .397	.124 .224	.288* .004	−.379* .000	−.671* .000	−.092 .368	.115 .258
daily rainfall	Pearson P value	.787* .000	1	.975* .000	.283* .005	.276* .006	.017 .869	−.058 .572	.114 .263	.200 .048	−.154 .130	−.596* .000	−.132 .196	.086 .400
3 day rainfall	Pearson P value	.779* .000	.975* .000	1	.291* .004	.302* .003	.050 .627	−.060 .557	.137 .178	.202 .046	−.187 .066	−.571* .000	−.103 .312	.103 .312
distance to stream	Pearson P value	.453* .000	.283* .005	.291* .004	1	.668** .000	.052 .614	−.145 .153	.251 .013	.207 .041	−.668* .000	−.298* .003	.011 .916	.255 .011
elevation	Pearson P value	.516* .000	.276* .006	.302* .003	.668* .000	1	.038 .713	.079 .440	−.129 .207	.671* .000	−.616* .000	−.378* 000	−.090 .377	−.155 .127
slope	Pearson P value	−.017 .868	.017 .869	.050 .627	.052 .614	.038 .713	1	−.449* .000	.520* .000	−.303* .002	−.372* 0000	.134 .188	−.477* .000	.583* .000
plan curvature	Pearson P value	−.087 .397	−.058 .572	−.060 .557	−.145 .153	.079 .440	−.449* .000	1	−.864* .000	.282* .005	.195 .055	.068 .509	.080 .436	−.452* .000
profile curvature	Pearson P value	.124 .224	.114 .263	.137 .178	.251 .013	−.129 .207	.520* .000	−.864* .000	1	−.496* .000	−.355* .000	−.075 .463	−.103 .311	.709* .000
elevation of stream	Pearson P value	.288* .004	.200 .048	.202 .046	.207 .041	.671* .000	−.303* .002	.282* .005	−.496* .000	1	.171 .093	−.308* .002	.067 .509	−.550* .000
relative elevation	Pearson P value	−.379* .000	−.154 .130	−.187 .066	−.668* .000	−.616* .000	−.372* .000	.195 .055	−.355* .000	.171 .093	1	.175 .085	.191 .059	−.378* .000
TPI	Pearson P value	−.671* .000	−.596* .000	−.571* .000	−.298* .003	−.378* .000	.134 .188	.068 .509	−.075 .463	−.308* .002	.175 .085	1	−.063 .537	−.053 .606
TWI	Pearson P value	−.092 .368	−.132 .196	−.103 .312	.011 .916	−.090 .377	−.477* .000	.080 .436	−.103 .311	.067 .509	.191 .059	−.063 .537	1	−.114 .265
VRM	Pearson P value	.115 .258	.086 .400	.103 .312	.255 .011	−.155 .127	.583* .000	−.452* .000	.709* .000	−.550* .000	−.378* .000	−.053 .606	−.114 .265	1

Table 2 Independent variables used for multi-regression analysis

Independent variables	Description
X_{daily}	Daily precipitation (mm/day)
X_{accum}	3 day accumulated precipitation (mm/3days)
X_{stream}	Relative elevation to the nearest stream (m)
X_{tpi}	Topographic Position Index
$X_{elevation}$	Elevation of the location (m)
$X_{distance}$	Distance to stream (m)
$X_{ele\ stream}$	Elevation of the nearest stream (m)

Table 3 The results of multi-regression analysis with daily precipitation

	OLS				Quadratic			
	1	2	3	4	5	6	7	8
X_{daily}	.003 (.000)*	.003 (.000)*	.003 (.000)*	.003 (.000)*	.000 (.000)*	.000 (.000)*	.000 (.000)*	.000 (.000)*
X_{stream}	-.036 (.010)*	-.037 (.007)*	-.032 (.007)*	-	-.031 (.012)	-.033 (.008)*	-.028 (.008)*	-
X_{tpi}	-.014 (.004)*	-.014 (.004)*	-.017 (.004)*	-.019 (.004)*	-.023 (.004)*	-.023 (.004)*	-.025 (.004)*	-.026 (.005)*
$X_{ele\ stream}$	.018 (.010)	.019 (.007)	-	-	.015 (.009)	.016 (.008)	-	-
$X_{distance}$	.000 (.000)	-	-	-	.000 (.000)	-	-	-
$X_{elevation}$	Excluded	-	-	-	Excluded	-	-	-
R^2	.757	.757	.738	.682	.675	.675	.662	.620
F value	57.270	72.331	88.323	102.042	38.155	48.182	61.361	77.416

* Correlation is significant at the 0.01 level (2-tailed).

Table 4 The results of multi-regression analysis with accumulated precipitation

	OLS				Quadratic			
	1	2	3	4	5	6	7	8
X_{accum}	.004 (.000)*	.004 (.000)*	.004 (.000)*	.004 (.001)*	.000 (.000)*	.000 (.000)*	.000 (.000)*	.000 (.000)*
X_{stream}	-.031 (.011)*	-.034 (.007)*	-.030 (.007)*	–	-.028 (.012)	-.030 (.009)*	-.026 (.009)*	–
X_{tpi}	-.017 (.004)*	-.017 (.004)*	-.019 (.004)*	-.021 (.004)*	-.025 (.004)*	-.025 (.004)*	-.027 (.004)*	-.028 (.004)*
$X_{ele\ stream}$	.016 (.008)	.017 (.007)	–	–	.014 (.009)	.015 (.008)	–	–
$X_{distance}$	.000 (.000)	–	–	–	.000 (.000)	–	–	–
$X_{elevation}$	Excluded	–	–	–	Excluded	–	–	–
R^2	.745	.745	.720	.675	.662	.661	.649	.607
F value	53.778	67.768	84.097	101.902	35.979	45.399	57.999	75.807

* Correlation is significant at the 0.01 level (2-tailed).

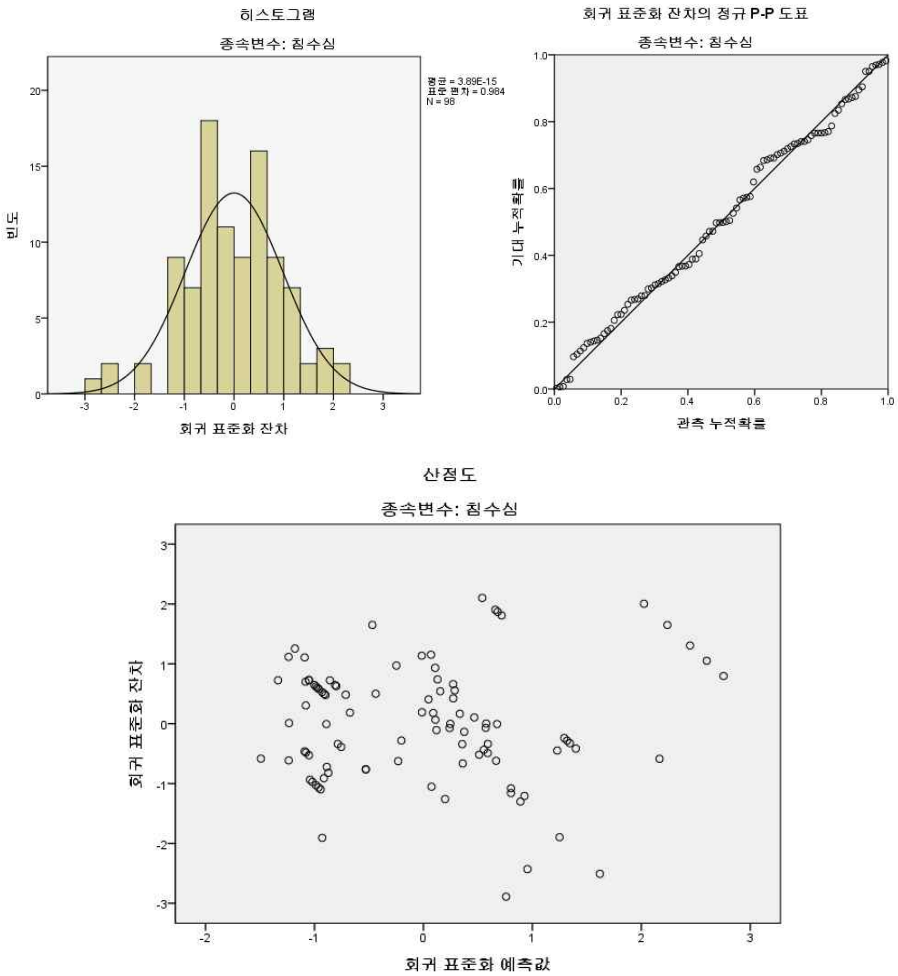

Fig. 1 Residual analysis of the model including daily precipitation

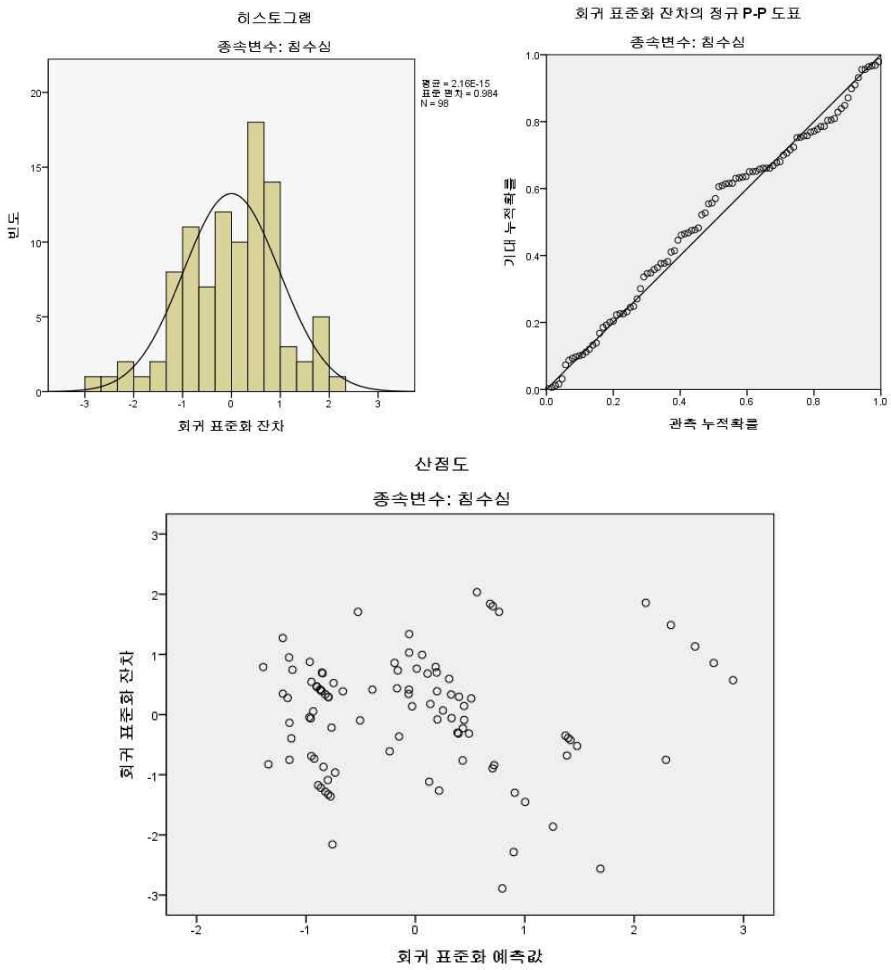

Fig. 2 Residual analysis of the model including accumulated precipitation

국문 초록

기후변화의 불확실성을 고려한 침수심에 따른 침수위험도 평가

김지연
서울대학교 농업생명과학대학원
생태조경·지역시스템공학부 생태조경학전공
지도교수: 이동근

도시 침수는 최근 가장 빈번하게 발생하고 있는 자연 재해 중 하나이다. 이는 기후변화에 따라 집중 호우의 빈도 및 강도가 증가하고 있기 때문이다. 실제로 서울을 비롯한 수도권 지역이 상습적으로 침수되고 있지만, 기개발지에서 침수 대응 시설이나 대책을 계속해서 공급하는 것은 한계가 있다. 따라서 향후 이루어질 도시 계획 단계에서 침수 위험을 미리 고려할 필요가 있다.

그러나 공간 계획에 반영하기 위한 침수위험도를 정량화함에 있어서 불확실성을 고려한 연구는 많지 않다. 또한 침수위험도를 나타내는 주요한 요소인 침수심은 복잡한 수리수문 모형으로부터 도출되어 실제로 그 결과를 활용해야 하는 계획가나 정책결정자가 접근하기 어려운 점이 있었다. 따라서 본 연구의 목적은 침수심 예측 모형을 개발하고 기후 시나리오의 불확실성을 고려한 침수위험도 평가를 하는 것이다.

연구 대상지는 각종 개발 사업이 추진 중이며 상습적으로 침수되어 도시 계획 시 침수위험도가 고려될 필요가 있는 김포시로 선정하였다. 본 연구는 다음과 같은 네 가지 부분으로 이루어졌다. 먼저, 기후 시나리오의 불확실성을 고려하도록 4개 RCP 시나리오의 앙상

블을 위한 몬테카를로 시뮬레이션을 수행하였다. 두 번째로, 다중회귀분석을 이용하여 침수심 예측 모형을 구축하였다. 세 번째로, 공간 통계모형인 MaxEnt를 이용하여 지형·물리적 요인에 따른 침수민감성을 파악하였다. 마지막으로 2050년의 잠재 침수심지도와 침수민감성 지도를 결합함으로써 침수위험도를 나타내었다.

RCP4.5, 8.5 시나리오에서는 2050년의 강우일수가 RCP2.6, 6.0 시나리오보다 약 2배 많으며, 3일 연속으로 비가 오는 날은 1.85배 많은 것으로 나타났다. 몬테카를로 시뮬레이션에 의해 도출된 앙상블 시나리오로부터 2050년의 극한강수량이 증가할 것으로 나타났다. 일강우량과 3일 누적강우량의 평균값은 현재와 유사한 수준이었으나, 최댓값은 현재보다 각각 106.76mm, 55.66mm만큼 증가함을 보였다.

침수심 예측모형을 구성하는 변수는 일강우량, 3일 누적강우량, 가장 가까운 하천과의 고도 차이, 지형위치지수(TPI)로 선정되었다. 침수심 예측모형에 2050년 강우량을 적용시킨 결과, 김포시에서 미래 일강우량에 의한 침수심이 가장 낮은 지역은 0.01−0.05m로 나타났으며, 가장 높은 지역은 1.64−2.34m로 나타났다. 누적강우량을 고려할 경우 일강우량일 때 보다 침수심은 더 높게 나타났다.

지형·물리적으로 침수에 취약한 지역을 나타내는 침수민감성은 8개로 등급화하여 8등급을 가장 높은 침수민감성을 갖는 지역으로 나타내었다. 5−8등급에 해당하는 지역은 침수가 발생할 가능성이 있는 지역으로서 김포시의 28%를 차지하였다. 7등급에 해당하는 지역 중 침수심이 1.0m 이상 나타날 것으로 예상되는 지역은 7,200m^2 이다. 침수심이 1.0m 이상인 지역은 어떤 토지이용으로 할당되더라도 취약하기 때문에 도시 계획 시 이를 고려하여 개발지를 분류해야 할 것이다.

기후변화 시대를 살아가는 현대인들에게 있어 도시 계획의 새로

운 패러다임은 기후변화 영향을 줄이고 적응할 수 있도록 재해위험도 평가가 선행되어야 하는 것이라고 할 수 있다. 본 연구의 의의는 미래의 다양한 기후변화 시나리오를 적용하여 기후변화에서 비롯되는 불확실성을 반영한 의사결정을 지원할 수 있다는데 있다. 이는 계획가 및 정책결정자로 하여금 보다 합리적인 판단을 내리는데 도움이 될 수 있다. 뿐만 아니라, 본 연구에서 제시한 침수심 예측 모형은 계획가 및 정책결정자도 쉽게 파악하여 이용할 수 있어 침수위험을 계획에 반영하는데 실질적인 기여를 할 것으로 생각된다.

■ 주요 용어: 침수심, 침수민감성, 강우 확률분포, 극한 강우사상, 침수 적응 대책, 공간 계획

■ 학 번: 2013-21146